JACC Vol. 46, No. 5, 2005
September 6, 2005:799–806

Reprint requests and correspondence: Dr. Luciano Cominacini, Dipartimento di Scienze Biomediche e Chirurgiche, Sezione di Medicina Interna D - Università di Verona, Policlinico G.B. Rossi - P.le L.A. Scuro 10, 37134 Verona, Italy. E-mail: luciano.cominacini@univr.it.

REFERENCES

1. Libby P. Inflammation in atherosclerosis. Nature 2002;420:868–74.
2. Barnes PJ, Karin M. Nuclear factor-kB—a pivotal transcriptional factor in chronic inflammatory diseases. N Engl J Med 1997;336: 1066–71.
3. Lenardo MJ, Baltimore D. NF-kB: a pleiotropic mediator of inducible and tissue-specific gene control. Cell 1989;58:227–9.
4. Beg AA, Baldwin AS. The IkB proteins: multifunctional regulators of Rel/NF-kB transcription factors. Genes Dev 1993;7:2061–70.
5. Ross R. The pathogenesis of atherosclerosis: a perspective for the 1990s. Nature 1993;362:801–9.
6. Brand K, Eisele T, Kreusel U, et al. Dysregulation of monocytic nuclear factor-kB by oxidized low-density lipoprotein. Arterioscl Thromb Vasc Biol 1997;17:1901–9.
7. Wilson SH, Bets PJM, Edwards WD, et al. Nuclear factor-kB immunoreactivity is present in human coronary plaque and enhanced in patients with unstable angina pectoris. Atherosclerosis 2002;160: 147–53.
8. Ritchie ME. Nuclear factor-kB is selectively and markedly activated in humans with unstable angina pectoris. Circulation 1998;98:1707–13.
9. Holvoet P, Vanhaecke J, Janssens S, Van de Werf F, Collen D. Oxidized LDL and malondialdehyde-modified LDL in patients with acute coronary syndromes and stable coronary artery disease. Circulation 1998;98:1487–94.
10. Nishi K, Itabe H, Uno M, et al. Oxidized LDL in carotid plaques and plasma associates with plaque instability. Arterioscler Thromb Vasc Biol 2002;22:1649–54.
11. Ehara S, Ueda M, Naruko T, et al. Elevated levels of low density lipoprotein show a positive relationship with the severity of acute coronary syndromes. Circulation 2001;103:1955–60.
12. Horiuchi S, Sakamo Y, Sakai M. Scavenger receptors for oxidized and glycated proteins. Amino Acids 2003;25:283–92.
13. Kunjathoor VV, Febbraio M, Podrez EA, et al. Scavenger receptors class A-I/II and CD36 are the principal receptors responsible for the uptake of modified low density lipoprotein leading to lipid loading in macrophages. J Biol Chem 2002;277:49982–8.
14. Kita T, Kume N, Minami M, et al. Role of oxidized LDL in atherosclerosis. Ann N Y Acad Sci 2001;947:199–205.
15. Cominacini L, Pasini AF, Garbin U, et al. Oxidized low density lipoprotein (ox-LDL) binding to ox-LDL receptor-1 in endothelial cells induces the activation of NF-kappaB through an increased production of intracellular reactive oxygen species. J Biol Chem 2000;275:12633–8.
16. Braunwald E. Unstable angina: a classification. Circulation 1989;80: 410–4.
17. Boyum A. Isolation of mononuclear cells and granulocytes from human blood. Scand J Clin Lab 1968;21 Suppl 97:77–89.
18. Renard P, Ernest I, Houbion A, et al. Development of a sensitive multi-well colorimetric assay for active NF-kB. Nucleic Acids Res 2001;29:E21.
19. Ichiyama T, Nishikawa M, Yoshitomi T, et al. Clarithromicin inhibits NF-kB activation in human peripheral blood mononuclear cells and pulmonary epithelial cells. Antimicrob Agents Chemother 2001;45:44–7.
20. Holvoet P, Stassen JM, Van Cleeput J, Collen D, Vanhaecke J. Oxidized low density lipoproteins in patients with transplant-associated coronary artery disease. Arterioscler Thromb Vasc Biol 1998;18:100–7.
21. Havel RJ, Eder MA, Bragdon JM. The distribution and chemical composition of ultracentrifugally separated lipoproteins in human serum. J Clin Invest 1955;34:1345–53.
22. Sawamura T, Kume N, Aoyama T, et al. An endothelial receptor for oxidized low-density lipoprotein. Nature 1997;386:73–7.
23. Tsimikas S, Bergmark C, Beyer RW, et al. Temporal increases in plasma markers of oxidized low-density lipoprotein strongly reflect the presence of acute coronary syndromes. J Am Coll Cardiol 2003;41:360–70.
24. Yamanaka S, Zhang XY, Miura K, Kim S, Iwao H. The human gene encoding the lectin-type oxidized LDL receptor (OLR1) is a novel member of the natural killer gene complex with a unique expression profile. Genomics 1998;54:191–9.

ELSEVIER

Atherosclerosis xxx (2005) xxx–xxx

ATHEROSCLEROSIS

www.elsevier.com/locate/atherosclerosis

Low-density lipoprotein oxidized to various degrees activates ERK1/2 through Lox-1

Hiroyuki Tanigawa [a], Shin-ichiro Miura [a,*], Bo Zhang [a], Yoshinari Uehara [a], Yoshino Matsuo [a], Masahiro Fujino [a], Tatsuya Sawamura [b], Keijiro Saku [a]

[a] *Department of Cardiology, Fukuoka University Hospital, Fukuoka, Japan*
[b] *Department of Bioscience, National Cardiovascular Center Research Institute, Osaka, Japan*

Received 18 April 2005; received in revised form 20 October 2005; accepted 26 October 2005

Abstract

Although the standard procedure for preparing extensively oxidized low-density lipoprotein (Ox-LDL) is to incubate it with 10 μM $CuSO_4$ at 37 °C for 24 h, it is not well known how important the degree of oxidation of LDL is for inducing cell signaling. Since Lox-1 (an Ox-LDL receptor) contributes to cell proliferation through extracellular-signal-regulated kinase (ERK)1/2 activation and subsequently induces plaque growth, we analyzed ERK activity using LDL with various degrees of oxidation, from minimally Ox-LDL, which is mainly in human plasma, to extensively Ox-LDL using capillary electrophoresis (cITP). The cITP was a suitable tool for evaluating the degree of oxidation of LDL for analyzing the optimal conditions for the oxidation of LDL by $CuSO_4$ to obtain LDL that was oxidized to a degree comparable to that in human plasma. In addition, both minimally and extensively Ox-LDL induced similar levels of ERK1/2 activation through Lox-1 in human coronary artery smooth muscle cells. These results indicate that both minimally and extensively Ox-LDL may be important for the progression of plaque growth through Lox-1. Since most previous reports have provided data only using extensively Ox-LDL, a re-evaluation is needed to analyze several signals that use LDL which has been oxidized to various degrees.

Keywords: Low-density lipoprotein; Oxidiation; Extracellular-signal-regulated kinase; Lox-1; Capillary electrophoresis

Oxidized low-density lipoprotein (Ox-LDL) is widely believed to play an important role in the pathogenesis of atherosclerosis. Oxidized LDL may be endocytosed by macrophages, resulting in the generation of cholesterol-laden foam cells, which characterize atherosclerotic lesions [1,2]. Ox-LDL is also chemotactic for leukocytes, is cytotoxic, can induce smooth muscle cell proliferation, and has many other potentially atherogenic effects. Lox-1, which is an oxidized low-density lipoprotein (Ox-LDL) receptor, has been associated with the activation of extracellular-signal-regulated kinase (ERK)1/2. Native LDL and LDL oxidized by the addition of Cu^{2+} stimulated ERK1/2 in a time- and dose-dependent manner in rat vascular smooth muscle cells (VSMCs), and the maximal ERK1/2 response to Cu^{2+}-oxidized LDL was significantly greater than the response to native LDL [3]. Although Ox-LDL activates ERK1/2 [3–5], it is not known whether the degree of oxidation of LDL is important for inducing ERK activation.

The oxidative modification of trapped lipoproteins was originally proposed in the early 1980s [6]. Steinbrecher et al. reported that when incubation conditions in the absence of cells were selected to favor oxidation, for example, by extending the duration of incubation of LDL at low concentrations, or by increasing the Cu^{2+} concentration, LDL underwent changes very similar to those that occur in the presence of cells, including degradation of phosphatidylcholine [7]. They also reported that the oxidation of LDL by exposure to 5 μM $CuSO_4$ at 37 °C for 20 h resulted in a modification that was indistinguishable from that produced by endothelial

* Corresponding author at: Department of Cardiology, Fukuoka University Hospital, 7-45-1 Nanakuma, Jonan-ku, Fukuoka 814-0180, Japan.
Tel.: +81 92 801 1011; fax: +81 92 865 2692.
E-mail address: miuras@cis.fukuoka-u.ac.jp (S.-i. Miura).

0021-9150/$ – see front matter © 2005 Elsevier Ireland Ltd. All rights reserved.
doi:10.1016/j.atherosclerosis.2005.10.046

cells [8], and the modification of LDL by oxidation using $CuSO_4$ has been shown to permit recognition by the SR-A of macrophages [9]. Recently, the standard procedure for preparing extensively Ox-LDL was to incubate it with 10 μM $CuSO_4$ at 37 °C for 18 h [10–12].

Oxidative modification of LDL is a complex process and is accompanied by the production of thiobarbituric acid-reactive substances (TBARS) [7], increased agarose gel electrophoretic mobility, and an increased buoyant density of lipoprotein particles [13]. There have been dramatic improvements in electrophoresis and the evaluation of LDL by capillary electrophoresis has been reported [14]. Schmitz et al. reported that LDL is separated by capillary isotachophoresis (cITP) into two major subpopulations [15]. Zorn et al. presented the first study to investigate LDL-subfractions separated by cITP and the changes in these LDL-subfractions after gradual in vitro oxidation and after oxidative modification by monocyte-derived macrophages and vascular smooth muscle cells (VSMCs) [16]. However, there has been no report on whether Ox-LDL made by $CuSO_4$ shows a different degree of oxidation than Ox-LDL in human plasma as assessed by cITP.

Therefore, we analyzed the degree of Ox-LDL produced by $CuSO_4$ using cITP, agarose electrophoresis and TBARS, and then established optimal conditions for the oxidation of LDL comparable to that in human plasma. We also determined the activation of ERK1/2 through Lox-1 in human coronary artery SMCs (HCSMCs) by LDL with different degrees of oxidation. In this study, we demonstrated that cITP is a suitable tool for analyzing the degree of oxidation and there were no differences in the strength of ERK1/2 activation induced by LDL with different degrees of oxidation in HCSMCs.

1. Methods

1.1. Lipoprotein preparation

LDL was isolated from fresh plasma obtained from a healthy volunteer by sequential ultracentrifugation as a $1.019 < d < 1.063$ g/ml fraction at 4 °C in potassium bromide [17]. The isolated LDL was dialyzed at 4 °C in slide-A-lyzer dialysis cassettes (Pierce) against 0.15 M sodium chloride with 1 mM ethylenediamine-*N*,*N*,*N*′,*N*′-tetraacetic acid, disodium salt, dihydrate (EDTA), pH 7.4, and before oxidization, LDL was dialyzed in slide-A-lyzer dialysis cassettes against phosphate-buffered saline (PBS), pH 7.4, at 4 °C with three changes in 24 h in the dark to remove EDTA.

1.2. Assessment of LDL oxidization

LDL (100 μg/ml) was incubated with 10 μM $CuSO_4$ in PBS buffer (pH 7.4) at 37 °C [11,12]. The time-course of Cu-induced oxidization of LDL was monitored continuously up to 24 h by cITP, agarose gel electrophoresis and TBARS. cITP was performed on a Beckman P/ACE MDQ system (Beckman-Coulter Inc.) according to the method of Bottcher et al. [18] with some modifications [19]. Agarose gel electrophoresis and differential staining were performed using a rapid electrophoresis system (REP, Helena Laboratories) according to the method of Kido et al. [20]. REP Lipo-30 plate and CHOL/TRIG COMBO (K.K. Helena Kenkyujo) were used as agarose gel and staining reagents, respectively. TBARS were measured by the method of Kojima et al. [21]. EDTA (100 μM) was added immediately for each Ox-LDL, and they were used for experiments within a day.

1.3. Cell culture

HCSMCs from the subject with normal coronary artery (Clonetics Corp.) were grown with SMC basal growth medium with 0.05 μg/ml human recombinant epidermal growth factor, 5 μg/ml insulin, 0.01 μg/ml human recombinant fibroblast growth factor, 10 μg/ml gentamicin, 0.05 μg/ml amphotericin-B and 5% fetal bovine serum (FBS) at 37 °C with 5% CO_2. HCSMCs expressed Lox-1 assessed by RT-PCR. HCSMCs were grown under SMC medium without FBS for 24 h before Ox-LDL treatment. To examine the receptor-specificity of Ox-LDL, HCSMCs were pretreated with human Lox-1 blocking antibody (Jmab92, 10 μg/ml) for 30 min and exposed to Ox-LDL [22].

1.4. Immunoblotting analysis for ERK

Cells harvested after treatment with or without Ox-LDL for 10 min were used to measure the expression of ERK1/2 activity. Cell lysate from each experiment was separated by 10% SDS-PAGE and transferred to nitrocellulose membranes. After incubation in blocking solution, membranes were incubated with primary antibody overnight at 4 °C. Membranes were washed, incubated with secondary antibody for 1 h, and then detected with the ECL system (Amersham). The levels of ERK1/2 were detected by ERK1/2 antibody (1:1000, Invitrogen, #9102) and phospho-ERK1/2 antibody (1:500, Invitrogen, #9106S), followed by goat anti-mouse IgG (H + L) horseradish peroxidase conjugate (1:1000, Bio-Rad) or goat anti-rabbit IgG (H + L) alkaline phosphatase conjugate (1:1000, Bio-Rad), respectively. The bands were visualized using an LAS-3000 luminous image analyzer. To quantify the densitometry of the bands, the films were scanned and the density of each band was measured using Image Gauge Ver 4.0.

2. Results

2.1. Capillary electrophoresis of native LDL

Although the presence of Ox-LDL in human plasma was demonstrated by sandwich ELISA using DLH3 together with

an anti-apoB antibody, only the amount of Ox-LDL was determined, and not the degree of oxidation [23]. Therefore, we used cITP to analyze the degree of oxidation, and did not determine the amount of Ox-LDL in plasma. Fig. 1 shows a typical electropherogram of plasma lipoprotein subfractions as characterized by cITP, which can analyze the degree of oxidation, in 285 healthy subjects (our unpublished data). The cITP clearly separated lipoproteins into eight fractions within 8 min. The two LDL fractions with fast (peak 6) and slow (peak 7) electric mobility correspond to a small peak of electronegative LDL (minimally oxidized) and a large peak of native LDL [24].

2.2. *Changes in LDL electrophoretic mobility during Cu^{2+}-catalyzed oxidation by TBARS, agarose electrophoresis and capillary electrophoresis*

Since the degree of Ox-LDL in human plasma was not known, it was monitored by the electrophoretic mobility of LDL during Cu^{2+}-catalyzed oxidation by cITP. The optimal migration time was identified based on the peak of the electronegative LDL fraction. Since cITP separates plasma lipoproteins based on electric mobility, the electronegative LDL fraction carries a more negative electric mobility (extensively Ox-LDL). The electronegative LDL fraction could be

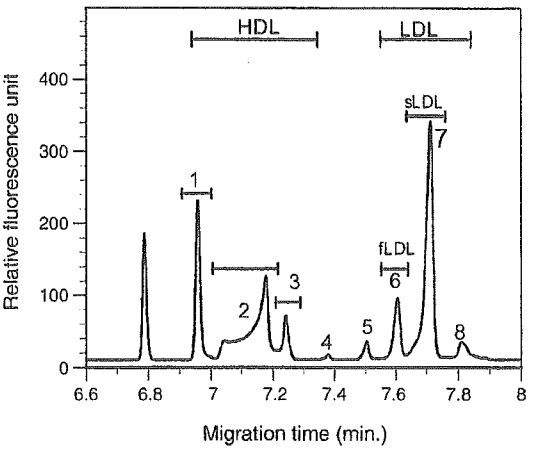

Fig. 1. A typical electropherogram of plasma lipoprotein subfractions as assessed by capillary electrophoresis in a healthy subject. Lipoprotein profiles were characterized by eight peaks: peak 1 was fast-migrating high-density lipoprotein (HDL), peak 2 was intermediate-migrating HDL, peak 3 was slow-migrating HDL, peak 4 was chylomicrons and large very LDL (VLDL), peak 5 was small VLDL and intermediate density lipoprotein (IDL), peak 6 was fast migrating (f) LDL and oxidized LDL, peak 7 was slow-migrating (s) LDL, and peak 8 was a small LDL peak.

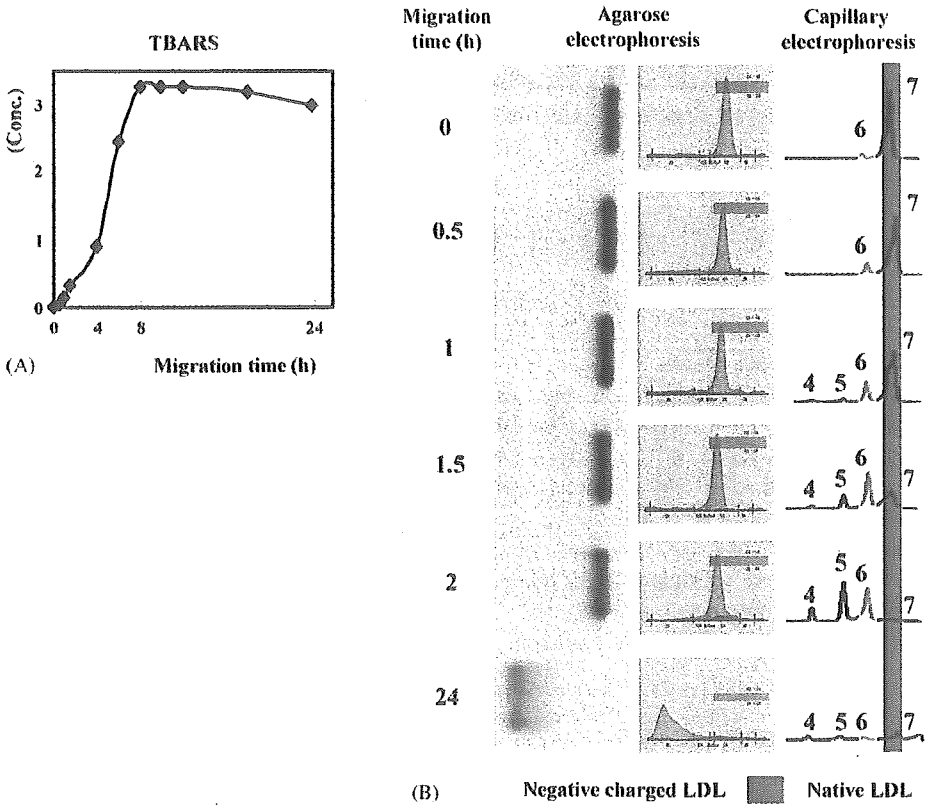

Fig. 2. (A) Change in the oxidation of LDL using 10 μM $CuSO_4$ as monitored by TBARS. (B) Change in the oxidation of LDL using 10 μM $CuSO_4$ as monitored by capillary electrophoresis and agarose electrophoresis.

an atherogenic LDL because the LDL fraction is inversely correlated with the size of LDL and increases with the oxidation of LDL (our unpublished data).

To evaluate the degree of oxidation of LDL, LDL was oxidized with 10 μM $CuSO_4$ at 37 °C, and monitored by TBARS, agarose electrophoresis and cITP. As shown in Fig. 2, Ox-LDL that was incubated for 1.5 h had the highest peak of electronegative LDL (peak 6) in human plasma as assessed by cITP, while the band was shifted a little bit in agarose electrophoresis and a lower concentration was observed in TBARS. In addition, the band with Ox-LDL that had been incubated for 24 h was strongly shifted by cITP. Massive and extensive oxidation that has conventionally been considered to be optimal was observed for Ox-LDL that had been incubated for 24 h with $CuSO_4$ in TBARS [7,25]. However, after 24 h of incubation, there was no peak of native LDL or Ox-LDL by cITP, and LDL showed a strong negative charge that does not normally exist in human plasma. Therefore, extensive Ox-LDL as assessed by agarose electrophoresis and TBARS does not exist in human plasma. To obtain minimally Ox-LDL comparable to Ox-LDL in human plasma, the optimal condition was incubation with 10 μM $CuSO_4$ for 1.5 h.

2.3. *Minimally Ox-LDL induces ERK1/2 activity via hLox-1*

Since native LDL and LDL extensively oxidized by $CuSO_4$ stimulated ERK1/2 in a time- and dose-dependent manner in baboon and rat VSMC through Lox-1 [3], we also analyzed ERK1/2 with regard to the time- and dose-dependent effects of minimally Ox-LDL in a CHO cell system. EGFP-hLox-1-WT cells were incubated with Ox-LDL (0–200 μg/ml) for 0–20 min to determine the activation of ERK1/2 (Fig. 3A and B). The optimal condition for maximum ERK1/2 activation was when cells were incubated with 100 μg/ml Ox-LDL for 10 min, and these cells were used in further experiments.

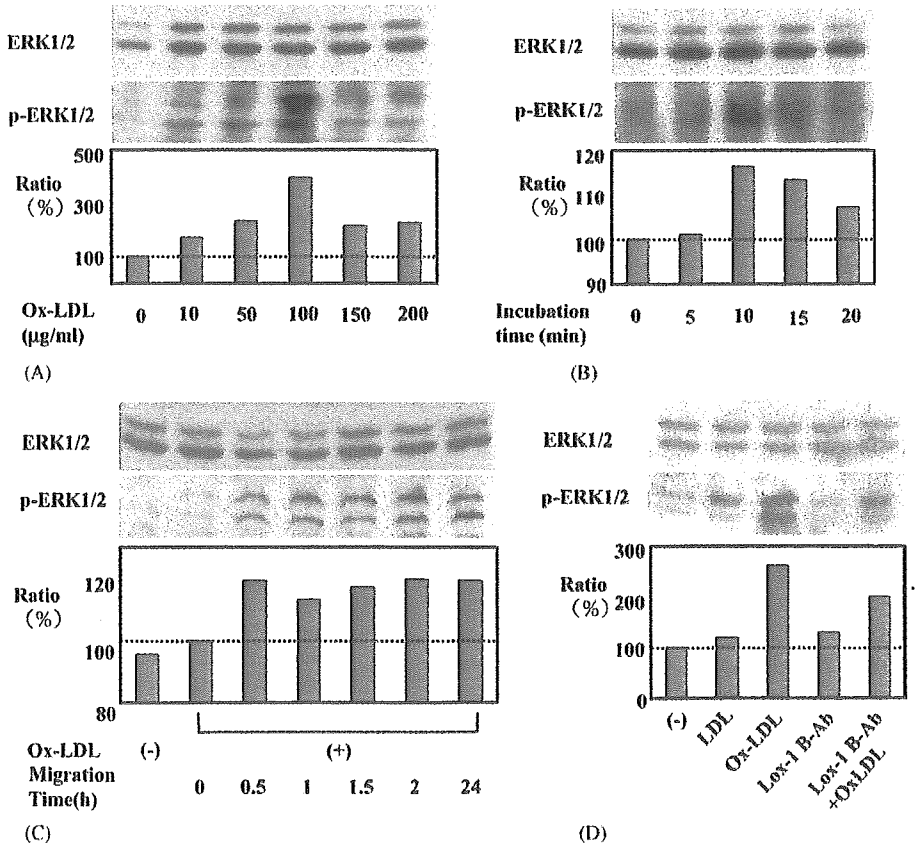

Fig. 3. CHO cells which stably expressed EGFP-Lox-1-WT were incubated with Ox-LDL (0–200 μg/ml) (A) for 0, 5, 10, 15, or 20 min (B). Cell lysates were analyzed by the immunoblotting method with ERK1/2 antibody and phosphorylation (p) of ERK1/2 antibody. We found that cells incubated with 100 μg/ml Ox-LDL for 10 min showed maximal p-ERK1/2, and they were used in subsequent experiments. (C) LDL that had been oxidized to different degrees using $CuSO_4$-induced ERK1/2 activation in human HCSMCs. The cells were incubated for 10 min with Ox-LDL that had been obtained using 10 μM $CuSO_4$ for the indicated migration times (0, 0.5, 1, 1.5, 2 and 24 h). (D) Ox-LDL obtained using $CuSO_4$ induced ERK1/2 activation through Lox-1 in HCSMCs. The cells were incubated for 10 min with or without 100 μg/ml LDL or 100 μg/ml Ox-LDL that was obtained using 10 μM $CuSO_4$ for 1.5 h of migration. Lox-1 blocking antibody (Lox-1 B-Ab) also preincubated for 1 h. The graph shows the % ratio of p-ERK to ERK in each sample relative to 100% for the control sample. Representative immunoblots (A–D) are shown. Three independent determinations were performed and similar results were observed (A–D).

2.4. Comparison of ERK1/2 activity induced by LDL with different degrees of oxidation and activation was through Lox-1

To study the effect of differences in the degree of oxidization on signal transduction of Lox-1, we compared ERK1/2 activation using Ox-LDL prepared using different durations of incubation with 10 μM $CuSO_4$. Ox-LDL (oxidized by 10 μM $CuSO_4$ at 37 °C for 0, 0.5, 1, 1.5, 2 and 24 h) was incubated for 10 min in HCSMCs (Fig. 3C). Similar levels of ERK1/2 activation were observed from 30 min to 24 h of incubation with $CuSO_4$, suggesting that both minimally and extensively Ox-LDL induced similar levels of ERK1/2 activation through hLox-1. Minimally Ox-LDL also activated ERK1/2 through Lox-1 in HCSMC (Fig. 3C). Ox-LDL-induced ERK1/2 activation was partially inhibited by human Lox-1 blocking antibody (Fig. 3D), which is a selective inhibitor of Lox-1 for blocking Ox-LDL binding and uptake in Lox-1-expressing cells [26], suggesting that minimally Ox-LDL activated ERK1/2 through Lox-1 in HCSMC.

3. Discussion

In this study, we established the optimal conditions for obtaining minimally Ox-LDL, which exists in human plasma, using cITP, which is a good strategy for determining the degree of oxidation of LDL. Both minimally and extensively Ox-LDL induced similar levels of ERK1/2 activation. The ERK activation plays a role in cell proliferation and differentiation [27]. Ox-LDL-induced ERK1/2 activation associated with cell proliferation might be mediated through a Ras/Raf/ERK pathway in cultured rat VSMC [28,29]. In addition, Ox-LDL is an important risk factor in the formation of atherosclerotic plaques. In the present study, native and modified lipoproteins induced a rapid phosphorylation of ERK in HCSMCs. Our data are in general agreement with previous studies showing that native and Cu-oxidized LDL activated ERK1/2 in VSMC [3]. On the other hand, our study differs from those reported in the literature in that we studied the influence of different degrees of oxidization on signal transduction via Lox-1. Both minimally and extensively Ox-LDL induced similar ERK1/2 activation through hLox-1 in HCSMCs in this study, while native and mildly modified LDL are more potent activators of ERK in VSMC than heavily modified LDL [30]. This inconsistency may be due to the different methods used to evaluate the degree of oxidation.

Although we only analyzed Lox-1 as an Ox-LDL receptor in this study, scavenger receptors also bind and internalize modified lipoproteins. There are several different classes of scavenger receptors, SR-A, SR-BI, SR-C, CD68, Lox-1 and SR-EC, in mammalian cells and they make various contributions to lipid transport. Other scavenger receptors also mediate cell signaling: for example, SR-BI induced endothelial nitric oxide synthase through src-PI3 kinase [31]. Although the main function of scavenger receptors is to regulate lipid transport, we also need to further investigate their role in cell signaling. In addition, since LDL showed variations in size and electronegativity compared to plasma LDL from aortic lesions in humans [32] and Watanabe rabbits [26], we also need to analyze the degree of oxidation of LDL by cITP in the vascular wall and measure ERK activity.

The cITP is a useful strategy for evaluating the degree of oxidation of LDL for analyzing the optimal conditions for the oxidation of LDL by $CuSO_4$ to obtain LDL that is oxidized to a degree comparable to that in human plasma. In addition, there were no differences in the strength of signaling induced by LDL with different degrees of oxidation. Since most previous reports have provided data only using extensively Ox-LDL, a re-evaluation is needed to analyze signaling using LDL that has been oxidized to various degrees in an in vitro study.

References

[1] Berliner JA, Heinecke JW. The role of oxidized lipoproteins in atherogenesis. Free Radic Biol Med 1996;20:707–27.
[2] Steinberg D. Low density lipoprotein oxidation and its pathobiological significance. J Biol Chem 1997;272:20963–6.
[3] Kusuhara M, Chait A, Cader A, Berk BC. Oxidized LDL stimulates mitogen-activated protein kinases in smooth muscle cells and macrophages. Arterioscler Thromb Vasc Biol 1997;17:141–8.
[4] Bjorkerud B, Bjorkerud S. Contrary effects of lightly and strongly oxidized LDL with potent promotion of growth versus apoptosis on arterial smooth muscle cells, macrophages, and fibroblasts. Arterioscler Thromb Vasc Biol 1996;16:416–24.
[5] Bachem MG, Wendelin D, Schneiderhan W, et al. Depending on their concentration, oxidized low density lipoproteins stimulate extracellular matrix synthesis or induce apoptosis in human coronary artery smooth muscle cells. Clin Chem Lab Med 1999;37: 319–26.
[6] Fogelman AM, Shechter I, Seager J, et al. Malondialdehyde alteration of low density lipoproteins leads to cholesteryl ester accumulation in human monocyte-macrophages. Proc Natl Acad Sci USA 1980;77:2214–8.
[7] Steinbrecher UP, Parthasarathy S, Leake DS, Witztum JL, Steinberg D. Modification of low density lipoprotein by endothelial cells involves lipid peroxidation and degradation of low density lipoprotein phospholipids. Proc Natl Acad Sci USA 1984;12:3883–7.
[8] Steinbrecher UP, Witztum JL, Parthasarathy S, Steinberg D. Decrease in reactive amino groups during oxidation or endothelial cell modification of LDL. Correlation with changes in receptor-mediated catabolism. Arteriosclerosis 1987;7:135–43.
[9] Steinbrecher UP. Oxidation of human low density lipoprotein results in derivatization of lysine residues of apolipoprotein B by lipid peroxide decomposition products. J Biol Chem 1987;262:3603–8.
[10] Hoff HF, Whitaker TE, O'Neil J. Oxidation of low density lipoprotein leads to particle aggregation and altered macrophage recognition. J Biol Chem 1992;267:602–9.
[11] Mine S, Tabata T, Wada Y, et al. Oxidized low density lipoprotein-induced LFA-1-dependent adhesion and transendothelial migration of monocytes via the protein kinase C pathway. Atherosclerosis 2002;160:281–8.
[12] Zeng HH, Tu PF, Zhou K, Wang H, Wang BH, Lu JF. Antioxidant properties of phenolic diterpenes from *Rosmarinus officinalis*. Acta Pharmacol Sin 2001;22:1094–8.
[13] Henriksen T, Mahoney EM, Steinberg D. Enhanced macrophage degradation of low density lipoprotein previously incubated with cul-

tured endothelial cells: recognition by receptors for acetylated low density lipoproteins. Proc Natl Acad Sci USA 1981;78:6499–503.
[14] Stocks J, Miller NE. Capillary electrophoresis to monitor the oxidative modification of low density lipoproteins. J Lipid Res 1998;39:1305–9.
[15] Schmitz G, Mollers C, Richter V. Analytical capillary isotachophoresis of human serum lipoproteins. Electrophoresis 1997;18:1807–13.
[16] Zorn U, Haug C, Celik E, et al. Characterization of modified low density lipoprotein subfractions by capillary isotachophoresis. Electrophoresis 2001;22:1143–9.
[17] Chapman MJ, Laplaud PM, Luc G, et al. Further resolution of the low density lipoprotein spectrum in normal human plasma: physicochemical characteristics of discrete subspecies separated by density gradient ultracentrifugation. J Lipid Res 1988;29:442–58.
[18] Bottcher A, Schlosser J, Kronenberg F, et al. Preparative free-solution isotachophoresis for separation of human plasma lipoproteins: apolipoprotein and lipid composition of HDL subfractions. J Lipid Res 2000:905–15.
[19] Zhang B, Noda K, Saku K. Effect of atorvastatin on total lipid profiles assessed by analytical capillary isotachophoresis. Cardiology 2003;99:211–3.
[20] Kido T, Kurata H, Matsumoto A, et al. Lipoprotein analysis using agarose gel electrophoresis and differential staining of lipids. J Atheroscler Thromb 2001;8:7–13.
[21] Kojima T, Kikugawa K, Kosugi H. Is the thiobarbituric acid-reactivity of blood plasma specific to lipid peroxidation? Chem Pharm Bull 1990;38:3414–8.
[22] Chen H, Li D, Saldeen T, Mehta JL. Transforming growth factor-beta(1) modulates oxidatively modified LDL-induced expression of adhesion molecules: role of Lox-1. Circ Res 2001;89:1155–60.
[23] Toshima S, Hasegawa A, Kurabayashi M, et al. Circulating oxidized low density lipoprotein levels. A biochemical risk marker for coronary heart disease. Arterioscler Thromb Vasc Biol 2000;20:2243–7.
[24] Zhang B, Tomura H, Kuwabara A, et al. Correlation of high density lipoprotein (HDL)-associated sphingosine 1-phosphate with serum levels of HDL-cholesterol and apolipoproteins. Atherosclerosis 2005;178:199–205.
[25] Noble RP. Electrophoretic separation of plasma lipoproteins in agarose gel. J Lipid Res 1968;9:693–700.
[26] Itabe H. Oxidized low-density lipoproteins: what is understood and what remains to be clarified. Biol Pharm Bull 2003;26:1–9.
[27] Robinson MJ, Cobb MH. Mitogen-activated protein kinase pathways. Curr Opin Cell Biol 1997;9:180–6.
[28] Yang CM, Chien CS, Hsiao LD, et al. Mitogenic effect of oxidized low-density lipoprotein on vascular smooth muscle cells mediated by activation of Ras/Raf/MEK/MAPK pathway. Br J Pharmacol 2001;132:1531–41.
[29] Sachinidis A, Seewald S, Epping P, et al. The growth-promoting effect of low-density lipoprotein may be mediated by a pertussis toxin-sensitive mitogen-activated protein kinase pathway. Mol Pharmacol 1997;52:389–97.
[30] Velarde V, Jenkins AJ, Christopher J, Lyons TJ, Jaffa AA. Activation of MAPK by modified low-density lipoproteins in vascular smooth muscle cells. J Appl Physiol 2001;91:1412–20.
[31] Mineo C, Shaul PW. HDL stimulation of endothelial nitric oxide synthase: a novel mechanism of HDL action. Trends Cardiovasc Med 2003;13:226–31.
[32] Daugherty A, Zweifel BS, Sobel BE, Schonfeld G. Isolation of low density lipoprotein from atherosclerotic vascular tissue of Watanabe heritable hyperlipidemic rabbits. Arteriosclerosis 1988;8:768–77.

ELSEVIER

Cardiovascular Research 69 (2006) 263 – 271

Cardiovascular Research

www.elsevier.com/locate/cardiores

Oxidized LDL receptor LOX-1 is involved in neointimal hyperplasia after balloon arterial injury in a rat model

Jun-ichi Hinagata [a,b], Makoto Kakutani [a], Takao Fujii [c], Takahiko Naruko [d], Nobutaka Inoue [a], Yoshiko Fujita [a], Jawahar L. Mehta [e], Makiko Ueda [c], Tatsuya Sawamura [a,b,*]

[a] *Department of Vascular Physiology, National Cardiovascular Center Research Institute, Suita, Osaka 565-8565, Japan*
[b] *Department of Molecular Pathophysiology, Graduate School of Pharmaceutical Sciences, Osaka University, Suita, Osaka 565-0871, Japan*
[c] *Department of Pathology, Osaka City University Medical School, Osaka 545-8585, Japan*
[d] *Department of Cardiology, Osaka City General Hospital, Osaka 534-0021, Japan*
[e] *Division of Cardiovascular Medicine, University of Arkansas Medical School, Little Rock, AR, United States*

Received 29 October 2004; received in revised form 14 August 2005; accepted 16 August 2005
Available online 22 September 2005
Time for primary review 31 days

Abstract

Objective: LOX-1 is a multi-ligand receptor originally identified as the endothelial oxidized LDL receptor. LOX-1 expression is also induced in smooth muscle cells in response to proinflammatory and oxidative stimuli. Here, we report on the role of LOX-1 in intimal hyperplasia, in which proinflammatory and oxidative stimuli are increased.
Methods and results: Left common carotid artery of rat was injured by a balloon catheter. The expression of LOX-1 was significantly increased within 24 h after the balloon injury and peaked at day 7. LOX-1 expression was observed predominantly in medial smooth muscle cells until day 3, and then shifted to predominantly intimal smooth muscle cells. At day 14, the expression was concentrated in the regenerated endothelial cells. To examine the contributory role of LOX-1 in the growth of intimal smooth muscle cells, rats were administered anti-LOX1 antibody intravenously every 3 days after balloon injury. Anti-LOX-1 antibody administration effectively suppressed intimal hyperplasia, oxidative stress, and leukocyte infiltration compared with control IgG. These findings suggest the importance of LOX-1 expression in the pathogenesis of neointimal formation in conjunction with oxidative stress and leukocyte infiltration.
Conclusion: The LOX-1 expressed in smooth muscle cells is involved in intimal hyperplasia in a rat model of balloon injury. Manipulation of LOX-1 activity is a novel potential therapeutic target to prevent restenosis after angioplasty.

Keywords: Restenosis; Neointimal formation; LOX-1; Smooth muscle cells

1. Introduction

Restenosis is a major complication after coronary angioplasty that occurs in 30% to 50% of patients within 6 months after the procedure [1]. Although the use of a stent significantly reduces the rate of restenosis, often the interventional procedures need to be repeated because of recurrent restenosis [2]. The major cause of restenosis is neointimal hyperplasia, which results from an excessive proliferative response of vascular smooth muscle cells (VSMC) to mechanical injury. This proliferative process includes VSMC activation, migration from media to the intima, and intimal growth [2,3].

There is a great deal of evidence to show the process of VSMC growth involves oxidative stress and inflammation related to the accumulation of leukocytes and platelets [4–8]. After injury to the vascular surface, attachment of platelets to the injured surface area and their activation/

* Corresponding author. Department of Vascular Physiology, National Cardiovascular Center research Institute, 5-7-1, Fujishirodai, Suita, Osaka, 565-8565, Japan. Tel.: +81 6 6833 5012x2518; fax: +81 6 6835 5329.
E-mail address: t-sawamura@umin.ac.jp (T. Sawamura).

0008-6363/$ - see front matter © 2005 European Society of Cardiology. Published by Elsevier B.V. All rights reserved.
doi:10.1016/j.cardiores.2005.08.013

aggregation occur almost immediately, and the migration of leukocytes follows. The platelets and leukocytes distributed in the injured blood vessel release reactive oxygen species and enhance oxidative stress on the vessel wall. These cells also release cytokines that induce the migration and proliferation of VSMCs. Mechanical stress to the vessel wall further contributes to the oxidative stress in VSMCs.

LOX-1 is a multiligand receptor, originally identified by our laboratory as the major OxLDL receptor in endothelial cells [9]. The expression of LOX-1 in endothelial cells is markedly increased in vitro by cytokines, such as tumor necrosis factor-α (TNF-α) and transforming growth factor-β_1(TGF-β_1) [10,11], and also is induced in vivo in hypertension, diabetes, and hyperlipidemia in animal models [12–14]. Ligand binding to LOX-1 induces superoxide generation, which is accompanied by a reduction of nitric oxide (NO) in endothelial cells. This is followed by the activation of transcription factors and the induction of the expression of adhesion molecules and chemokines [15–17]. These data suggest that LOX-1 over-expression promotes endothelial dysfunction and leads to pathological changes of blood vessels [18]. Recent studies have demonstrated that LOX-1 recognizes aged/apoptotic cells, activated platelets, and leukocytes [19–21]. As a leukocyte-adhesion molecule, LOX-1 is actually involved in inflammation, and an anti-LOX-1 antibody has been shown to suppress endotoxin-and zymosan-induced inflammation in an animal model [21,22]. Therefore, LOX-1 appears to be an important component of inflammation.

In addition to endothelial cells, LOX-1 is expressed in smooth muscle cells, macrophages, and platelets [23–25]. When the endothelium is injured and removed, as in the case of balloon induced injury, the LOX-1 expressed in smooth muscle cells and platelets could play an important pathophysiological role in events occurring in the vessel wall. To investigate this hypothesis, we examined whether LOX-1 is involved in the process of neointimal hyperplasia after balloon arterial injury.

2. Materials and methods

2.1. Preparation of lipoproteins

LDL (1.019–1.063 g/mL) was isolated by sequential ultracentrifugation from healthy human plasma as described previously [9]. LDL was oxidatively modified by exposing to 7.5 μM $CuSO_4$ for 16 h at 37 °C at the protein concentration of 3 mg/ml in phosphate-buffered saline (PBS). The degree of oxidation was estimated by measuring the amount of thiobarbituric acid-reactive substances (TBARS) and the relative electrophoretic mobility (REM) in agarose gel compared with native LDL. TBARS and REM values of OxLDL were 10.7 nmol/mg protein and 3.25, respectively. Labeling of OxLDL with 1,1′-dioctadecyl-3,3,3′3′-tetramethylindocarbocyanine perchlorate (DiI, Molecular Probes) was performed as described [9].

2.2. Cells

Rat LOX-1 cDNA [26] was subcloned into a mammalian expression vector pME18s. The plasmid was co-transfected with pSV2bsr carrying blasticidin S resistant gene into CHO-K1 cells as described [9]. CHO cells stably expressing rat LOX-1 (rat LOX-1-CHO) was selected and maintained under Ham's F12/10% fetal bovine serum and 10 μg/mL blasticidin S. Wild-type CHO-K1 cells were maintained under Ham's F12/10% fetal bovine serum.

2.3. Anti-LOX-1 antibody

Anti-LOX-1 monoclonal antibody was generated by immunizing mice with cells stably expressing bovine LOX-1 (bLOX-1-CHO). Hybridomas which produce antibody, JTX20, reactive to both bLOX-1 CHO and rat-LOX-1 CHO were selected for this purpose.

2.4. Immunofluorescent staining of culture cells

Culture cells were washed three times with PBS and fixed with 4% (v/v) paraformaldehyde in PBS for 10 min. Nonspecific reactions were blocked by incubating cells with 10% non-immune horse serum in PBS. Then, the cells were incubated with 5 μg/mL anti-LOX-1 antibody (JTX20) or non-immune mouse IgG in PBS containing 1%(w/v) BSA, and subsequently with biotinylated horse anti-mouse IgG (Vector Laboratories) in PBS containing 1%(v/v) horse serum according to the manufacturer's instruction. The cells were then incubated with streptavidin–fluorescein conjugate (Vector Laboratories) and subjected to observation with fluorescence microscopy.

2.5. Internalization of DiI-OxLDL by rat LOX-1-CHO

Rat LOX-1-CHO cells were incubated with 3 μg/mL DiI-OxLDL in Ham's F12, 10% newborn calf serum (NBCS, Gibco BRL) for 3 h at 37 °C. To observe the effects of antibody, anti-LOX-1 antibody or non-immune mouse IgG were added to the cells 5 min before the addition of DiI-OxLDL. The cells were washed three times with PBS to remove unbound DiI-OxLDL, and lysed in isopropanol. The fluorescence intensity of the cell lysate was determined by a fluorescence spectrophotometer (excitation: 530 nm, emission: 590 nm, Spectro Fluor, Tecan).

2.6. Animal experiments

The animal experiments in the present study conforms to the Guide for the Care and Use of Laboratory Animals published by the US National Institute of Health.

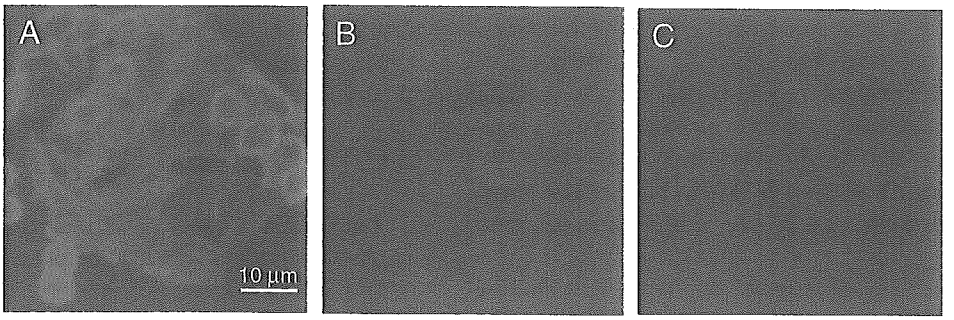

Fig. 1. Specificity of anti-LOX-1 antibody to rat LOX-1. Anti-LOX-1 antibody recognized CHO cells expressing rat LOX-1 (A) but not wild-type CHO cells (B). Non-immune mouse IgG did not recognize CHO cells expressing rat LOX-1 (C).

2.7. Clearance of anti-LOX-1 antibody after a bolus intravenous injection

Rats ($n=3$) were injected anti-LOX-1 antibody through tail vein at a dose of 10 mg/kg per rat. Blood (~0.1 mL) were collected from the tail vein at the indicated time points. To determine the plasma concentration of anti-LOX-1 antibody, sandwich enzyme immunoassay was performed by using anti-mouse IgG-Fc (Sigma) and horseradish peroxidase-conjugated anti-mouse immunoglobulin kappa chain (Southern biotechnology Associates, Inc.).

2.8. Arterial injury model

Male Sprague–Dawley rats weighing ~300 g were obtained from Japan SLC Inc. (Hamamatsu, Japan). Rats were anesthetized with pentobarbital (50 mg/kg, i.p.). The left common carotid artery was exposed under a surgical microscope. A deflated 2F balloon catheter (Fogarty, E-060-2F, Baxter) was inserted from external carotid artery and advanced to the aortic arch. An inflated balloon with 0.03 ml air was pull back toward the external carotid artery to denude the endothelium in common carotid artery. This process was repeated three times. Then, deflated catheter was pulled out, and the external carotid artery was ligated. At the indicated time points, the animals were sacrificed by injecting excess amount of anesthetic. The carotid arteries of the rats were perfused with phosphate-buffered saline (PBS), isolated, and excised into ~10 mm length (from the 5 mm proximal point from the internal–external branch), and then, snap-frozen in liquid nitrogen for RNA preparation, or in OCT

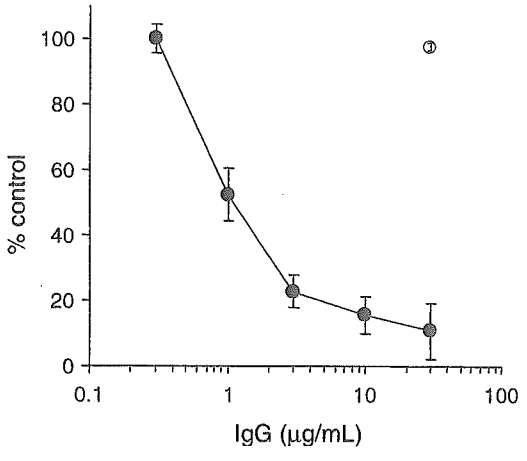

Fig. 2. Anti-LOX-1 antibody inhibits the binding and internalization of DiI-OxLDL. CHO cells stably expressing rat LOX-1 were incubated with indicated concentrations of anti-LOX-1 antibody (JTX20, ●), nonimmune IgG (○) and 3 μg/ml DiI-OxLDL in Ham's F12 with 10% NBCS for 3 h. The fluorescence intensity of DiI-OxLDL internalized by cells is expressed as a percentage of that in the absence of the antibody. Values are mean±SEM of three experiments in duplicate determinations.

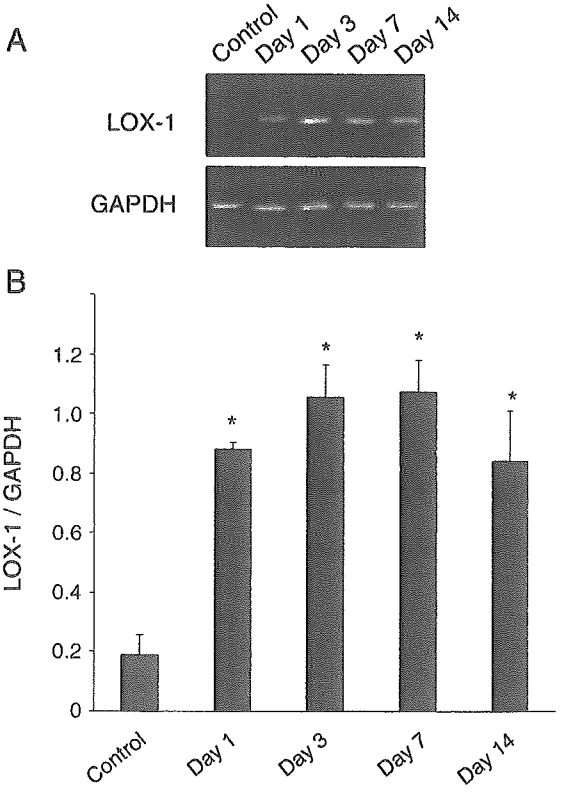

Fig. 3. (A) RT-PCR analysis of the expression of LOX-1 gene after balloon injury. Control displays mRNA level of LOX-1 before injury. (B) Densitometric analysis of the electrophoretic bands of the RT-PCR. Values are mean±SEM of the results ($n=4$ for control and day 1; $n=5$ for day 3, 7, and 14). *$P<0.01$ vs. control.

compound (Miles Laboratories) chilled by isopentan-dry ice for immunohistochemistry.

2.9. Reverse transcription-polymerase chain reaction (RT-PCR)

Total RNA was isolated from rat carotid arteries with Trizol reagent (Gibco BRL) according to manufacturer's manual. Total RNA (1 μg/mL per sample) was reverse transcribed with oligo $(dT)_{12-18}$ by SuperScript II reverse transcriptase (GIBCO BRL) at 42 °C for 1h. Five percent of the reaction was subjected to PCR using a primer pair specific to rat LOX-1 cDNA (forward primer: 5′-actcttc-aggtccttgtccaca-3′, reverse primer: 5′-gttgggatttttccgatgtaat-3′) in 35 thermal cycles of 94 °C for 40 s, 55 °C for 1 min, and 74 °C for 1 min to amplify 218 bp-product. GAPDH cDNA was amplified as internal control with forward primer: 5′-gcgcctggtcaccagggctgctt-3′, and reverse primer: 5′-tgccgaagtggtcgtggatgacct-3′) in 30 thermal cycles of 94 °C for 40 s, 60 °C for 1 min, and 74 °C for 1 min, to amplify 465 bp. The RT-PCR products were separated in 4% NuSieve 3:1 agarose gel (FMC bio-products) and visualized with ethidium bromide. The relative intensity of the bands was quantified using Scion Image software.

2.10. Immunohistochemistry

Left common carotid arteries were isolated and snap-frozen at 3, 7 and 14 days after balloon injury. The samples were sectioned serially at 6-μm thickness and fixed in acetone. Every first section was stained with hematoxylin-eosin; the other sections were used for immunohistochemical staining. The cellular components were analyzed by use of monoclonal antibodies against von Willebrand factor (1:1000, Dako A/S), myeloperoxidase (1:500, Abcam, Cambridge, UK), and LOX-1 (1 μg/mL). Sections were incubated at 4 °C overnight, and then subjected to a three-step staining procedure using the streptavidin-biotin complex method. Visualization was performed by horseradish peroxidase-based colorimetric reaction with 3-amino-9-ethyl-carbazole (10 min, room temperature), and the sections were faintly counterstained with hematoxylin.

2.11. Analyses of the effects of anti-LOX-1 antibody on the neointimal hyperplasia

Anti-LOX-1 antibody (10 mg/kg) or nonimmune mouse IgG (10 mg/kg) were administered intravenously to a subset of rats ($n=12$) immediately after balloon injury and every 3

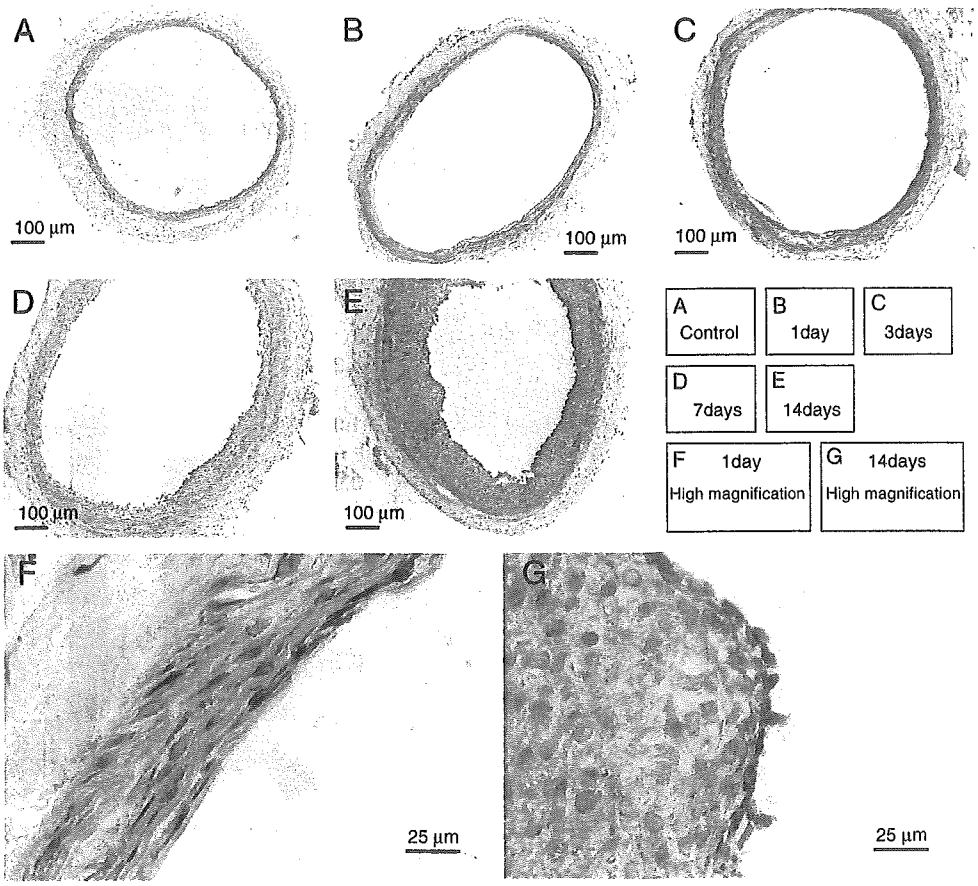

Fig. 4. Immunohistochemical detection of LOX-1 expression after balloon injury. Samples were collected before (A), and 1 (B and F), 3 (C), 7 (D), 14 day(s) (E and G) after balloon injury.

days thereafter. Fourteen days after the surgery, the carotid artery was isolated as described above. The carotid artery was fixed in 4%(w/v) formaldehyde and embedded in paraffin for histological analyses. Six 5 μm-thick sections from each carotid artery in interval of 2 mm were stained by the elastica van Gieson methods. Neointimal and medial areas were quantified with Scion Image software.

2.12. Detection of in situ generation of reactive oxygen species (ROS)

To detect in situ generation of ROS in the carotid artery specimens, fluorescence microphotography with dihydroethidium was performed as previously described [27,28]. Briefly, unfixed frozen samples were cut into 6 μm-thick sections and placed on glass slides. The slides were washed with PBS twice before loading dihydroethdium. Dihydroethidium (DHE, 10 μM) was applied to each tissue section, and then the sections were incubated in a light-protected chamber for 40 min. After washing with PBS, the image of dihydroethidium was obtained by a laser scanning confocal imaging system. Generation of ROS was demonstrated by red fluorescence labeling.

2.13. Statistics

All data are presented as mean±SEM. Difference of means was analyzed by two-tailed, unpaired Student's t test. Differences with P value less than 0.05 were considered significant.

3. Results

3.1. A neutralizing antibody against rat LOX-1

An anti-LOX-1 monoclonal antibody (JTX20) [29] that cross-reacts with rat LOX-1 was screened from a number of anti-bovine LOX-1 monoclonal antibodies [29]. The immunostaining of the CHO cell line expressing rat LOX-1 reveals the specificity of this antibody towards rat LOX-1

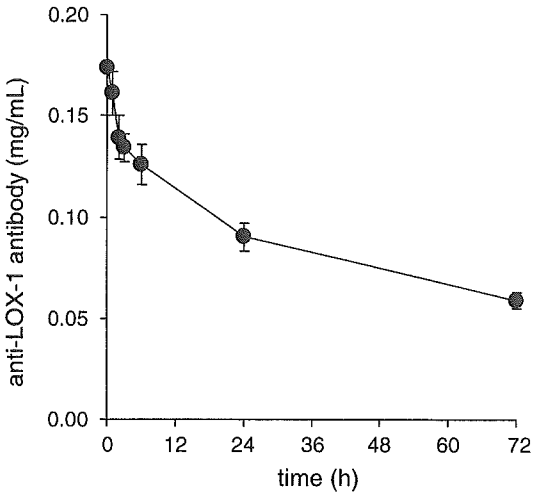

Fig. 6. Clearance of anti-LOX-1 antibody after single bolus intravenous injection (10 mg/kg). Data are mean±SEM (n=3).

(Fig. 1). JTX20 has exhibited potent neutralizing activity in various in vitro experiments; i.e., OxLDL binding and its biological responses, as well as the binding of platelets, bacteria, and advanced glycation endproducts [15,17,20, 29–32]. The epitope of the antibody involves the C-terminus of LOX-1, where the amino acid sequences are well conserved among the bovine, human, rat, porcine, rabbit, and rat [29] versions. JTX20 exhibited neutralizing activity against the internalization of fluorescently labeled OxLDL via rat LOX-1 (Fig. 2). Rat-LOX-1-CHO cells significantly incorporated DiI-OxLDL after incubation with 3 μg/ml DiI-OxLDL at 37 °C for 3 h. Anti-LOX-1 antibody blocked the uptake in a dose-dependent manner, while control IgG did not suppress the internalization even at 30 μg/mL. The IC_{50} value was approximately 1 μg/mL.

3.2. Effects of balloon injury on LOX-1 gene expression

Next, we analyzed the expression of LOX-1 after balloon injury, utilizing RT-PCR. As shown in Fig. 3, LOX-1 mRNA expression was markedly upregulated as early as 1 day after balloon injury in the injured left common carotid

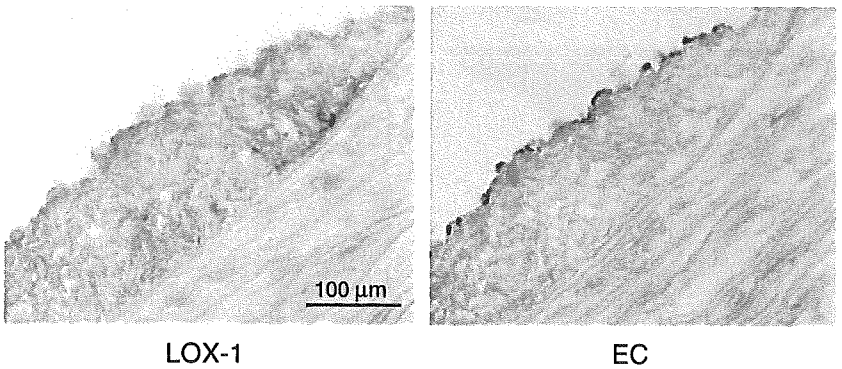

Fig. 5. Detection of regenerated endothelial cells 14 days after balloon injury. Endothelial cells were detected by anti-von Willebrand factor antibody. In the adjacent section, LOX-1 expression in the regenerated endothelial cells was observed as well as intimal smooth muscle cells.

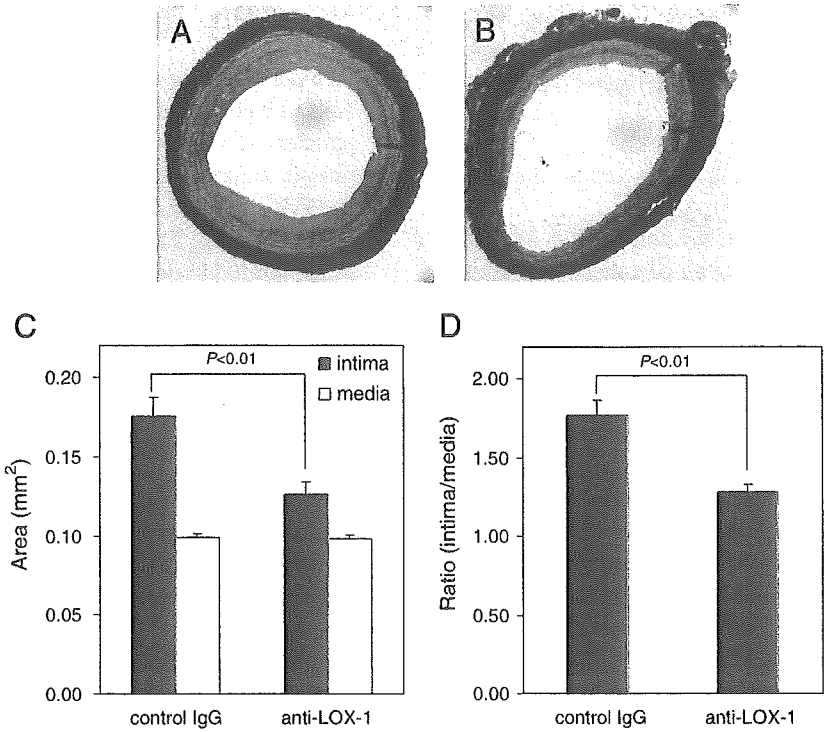

Fig. 7. Effects of the anti-LOX-1 antibody on neointimal formation in rat carotid arteries. Elastica van Gieson-staining of the cross section of injured artery treated with control IgG (A), and anti-LOX-1 antibody (B) are shown. (C) Intimal and medial area of the arteries at 14 days after injury. (D) Intimal/media ratio of the injured arteries. Data are mean±SEM from 12 rats. *$P<0.01$ vs. control IgG.

artery. The LOX-1 gene expression level was elevated 4-fold in the injured carotid artery in comparison with the uninjured artery ($P<0.01$). The genetic expression was induced over the entire 2-week observation after balloon injury, while it remained at the basal level in the control contra-lateral right common carotid artery (data not shown).

3.3. Localization of LOX-1 expressing cells in balloon-injured artery

The localization of LOX-1 expression in the carotid artery was determined by the immunostaining of serial sections with anti-rat LOX-1 antibody. In the control uninjured artery, LOX-1 protein was not detected (Fig. 4A). One day after balloon injury, LOX-1 was markedly expressed in medial smooth muscle cells (Fig. 4B and F). The expression of LOX-1 in smooth muscle cells gradually shifted from the media to the intima (Fig. 4C, D and E). In a section of the carotid artery 14 days after injury, while the LOX-1 expression was still evident in smooth muscle cells, a powerful expression of LOX-1 became observable in luminal endothelial cells (Fig. 4E and G). The localization of LOX-1 in the regenerated endothelial cells was confirmed by the staining of endothelial cells in the serial section with

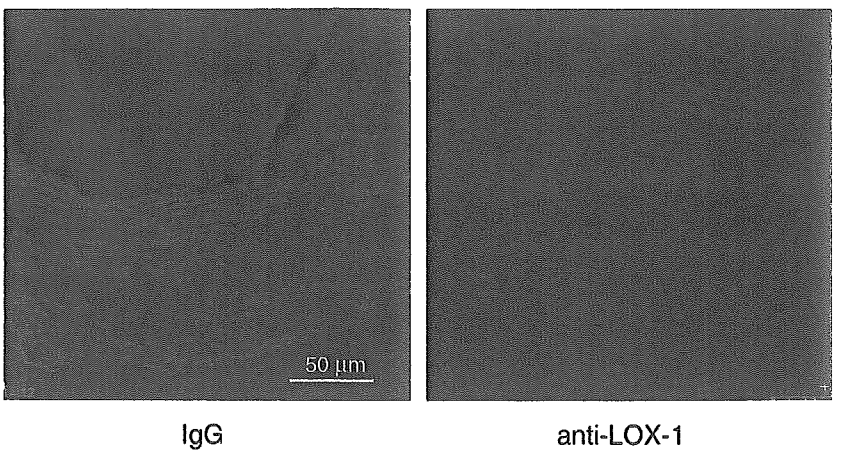

Fig. 8. Detection of in situ generation of reactive oxygen species (ROS). ROS generation were monitored by the oxidation of DHE on the sections from the injured arteries at day 7 treated with antiLOX-1 antibody or IgG.

anti-von Willebrand factor antibody (Fig. 5) In the intact right common carotid artery, the expression of LOX-1 was not detectable under the present immunostaining conditions (data not shown).

3.4. Effects of anti-LOX-1 antibody on intimal thickening

To examine the clearance of the anti-LOX-1 antibody in plasma, we administered 10 mg/kg of anti-LOX-1 antibody by bolus intravenous injection and determined the level of the antibody in the serum. The half-life of anti-LOX-1 antibody was determined to be approximately 24 h in the rat, which is shorter than the time determined by reports for mouse IgG [33–35] (Fig. 6). This might be due to the distribution of the antibody to LOX-1 expressed in vascular endothelial cells. In the dose administered to the rat, the serum anti-LOX-1 antibody level was maintained at >50 μg/ml over three days, which is sufficient to suppress the activity of rat LOX-1. Therefore, in order to suppress the increased activity of LOX-1 after balloon injury in a sustained manner, we administrated 10 mg/kg of anti-LOX-1 antibody every 3 days until the rats were sacrificed after 14 days.

Progressive intimal thickening in the injured left common carotid artery was observed 14 days after balloon injury in the control IgG-treated group. In contrast, the thickening was significantly suppressed in the injured left common carotid artery of rats treated with the anti-LOX-1 antibody (Fig. 7, A and B). Quantitative analyses of the thickened area showed that the neointimal area was reduced by 29.4%, and the intima to media ratio was reduced by 27.8% in the anti-LOX-1 antibody-treated group as compared with the control IgG-treated group (Fig. 7, C and D).

To clarify the mechanisms of the effects of the anti-LOX-1 antibody, we further analyzed the specimens 7 days after balloon injury. Analysis of in situ ROS generation detected by DHE revealed that the ROS level generated from the specimens of the anti-LOX-1-treated rat was markedly reduced compared with IgG-treated rats (Fig. 8). Furthermore, the leukocyte infiltration detected by immunostaining of myeloperoxidase was decreased in the injured artery of the anti-LOX-1 treated rat (Fig. 9).

4. Discussion

LOX-1 has been shown to be expressed in endothelial cells, macrophages, smooth muscle cells, and activated platelets [23–25,36]. LOX-1 expression can be induced by proinflammatory stimuli and oxidative stress, such as TNF-α, TGF-β, angiotensin II and reactive oxygen species [10,11,36–38]. These factors are thought to be important in neointimal hyperplasia after balloon injury [8,39–41]. In the present study, we demonstrated that balloon catheter injury induces LOX-1 expression and this enhances neointima formation. LOX-1 expression was induced in smooth muscle cells immediately after balloon injury. The localization of LOX-1 expression progressed with the pathological phases of neointima formation. In the early and intermediate phases, LOX-1 expression was localized in the medial and intimal smooth muscle cells, respectively, and in the advanced stages in the newly generated endothelial cells. The removal of endothelial cells appears to be involved in the induction of LOX-1 in VSMCs as these cells were exposed to proinflammatory cytokines and oxidative stress. Removal of endothelial cells leading to the decrease in endothelium-derived nitric oxide might also up-regulate the expression of LOX-1 in VSMCs, as reported in endothelial cells [42]. In addition, mechanical stimulation of VSMCs exposed to the shear stress of the flowing blood may also be involved, since fluid shear force has been shown to induce LOX-1 expression [43].

After mechanical injury/stimulation by the balloon catheter, cells in the arterial wall change their phenotype to the activated state [2]. In this sense, LOX-1 might be one of the immediate early genes that are induced on the stimulation of VSMCs. However, the significant suppression by anti-LOX-1 antibody of intimal hyperplasia suggests that LOX-1 might not be merely an inducible gene, but rather, might also be involved in the initiation and progression of the neointimal hyperplasia after balloon injury. It has been shown that the binding of ligands to LOX-1 induces oxidative stress, producing the superoxide anion. Oxidative stress, in turn, induces the expression of LOX-1 [38], forming a positive feedback loop [44], which

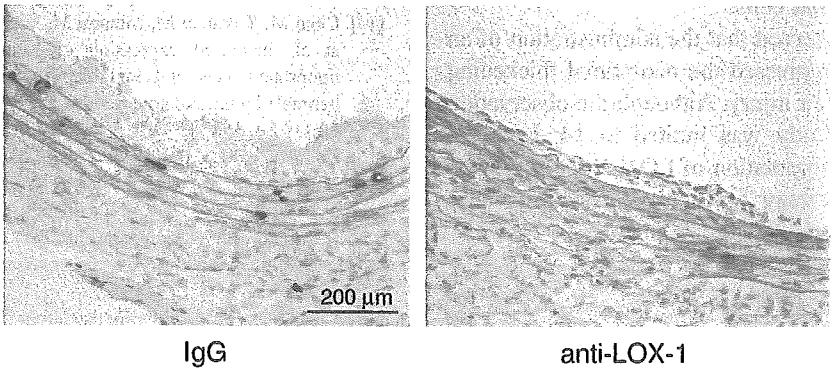

Fig. 9. Immunohistochemical detection of myeloperoxidase. Injured arteries at day 7 treated with antiLOX-1 antibody or IgG were stained with anti-myeloperoxidase antibody.

may contribute to the vicious cycle which characterizes the pathogenesis of intimal hyperplasia.

It has been reported that a potent anti-oxidative drug, probucol, inhibits neointimal formation in normocholesterolemic rabbits and porcine [45,46]. In the Multivitamins and Probucol (MVP) clinical trial, probucol was shown effective in reducing the rate of restenosis after balloon coronary angioplasty, although the cholesterol level was decreased in the probucol-treated group [47]. Furthermore, Muscoli et al. reported that a synthetic superoxide dismutase mimetic suppressed neointimal formation after balloon injury and suppressed the expression of LOX-1 in the developing lesion, although the evidence for the involvement of LOX-1 was indirect [48]. In the present study, blocking LOX-1 function with an anti-LOX-1 antibody actually reduced oxidative stress in the injured vascular wall. These findings support the importance of oxidative stress in neointimal formation in relationship with LOX-1.

As a multi-ligand receptor LOX-1 binds oxidized LDL, activated platelets, leukocytes, apoptotic cells and possibly other, as yet unidentified ligands. It is likely that LOX-1 interacts with these ligands on injured smooth muscle cells and increases the oxidative stress in the lesion which promotes intimal thickening. As a leukocyte adhesion molecule, LOX-1 has been shown to be involved in inflammation [21,22], one of the crucial factors in the pathogenesis of intimal hyperplasia. It is noteworthy that inflammation further enhances oxidative stress in the growing lesion. LOX-1 expression and activation may promote intimal thickening by promoting leukocyte attachment and the initiation of inflammation and oxidative stress. Actually, in the present study, the decrease in the infiltration of leukocytes as the result of treatment with the anti-LOX-1 antibody suggests the importance of the function of LOX-1 for leukocyte-adhesion.

In the final phase of pathological changes in the balloon-injured artery, marked expression of LOX-1 in the regenerated endothelium was observed two weeks after balloon injury. It has been reported that the regenerated endothelial cells exhibit an increased uptake of modified LDL and a reduced production of NO [49]. These findings may result from the up-regulated expression of LOX-1 in the regenerated endothelial cells.

In conclusion, we observed that the administration of an anti-LOX-1 antibody suppressed the neointimal thickening which occurs after balloon injury. Although the observation period in the present study was limited to 14 days, the findings suggest that manipulation of LOX-1 activity holds promise as a useful strategy to suppress restenosis after coronary intervention with a balloon catheter.

Acknowledgment

This work was supported in part by the grants from the Ministry of Education, Culture, Sports, Science and Technology of Japan; the Ministry of Health, Labor and Welfare of Japan, the Organization for Pharmaceutical Safety and Research. We thank Pacific Edit for reviewing the manuscript prior to publication.

References

[1] Landau C, Lange RA, Hillis LD. Percutaneous transluminal coronary angioplasty. N Engl J Med 1994;330:981–93.
[2] Bennett MR, O'Sullivan M. Mechanisms of angioplasty and stent restenosis: implications for design of rational therapy. Pharmacol Ther 2001;91:149–66.
[3] Nikol S, Huehns TY, Hofling B. Molecular biology and post-angioplasty restenosis. Atherosclerosis 1996;123:17–31.
[4] Welt FG, Rogers C. Inflammation and restenosis in the stent era. Arterioscler Thromb Vasc Biol 2002;22:1769–76.
[5] Hayashi S, Watanabe N, Nakazawa K, Suzuki J, Tsushima K, Tamatani T, et al. Roles of P-selectin in inflammation, neointimal formation, and vascular remodeling in balloon-injured rat carotid arteries. Circulation 2000;102:1710–7.
[6] Nguyen CM, Harrington RA. Glycoprotein IIb/IIIa receptor antagonists: a comparative review of their use in percutaneous coronary intervention. Am J Cardiovasc Drugs 2003;3:423–36.
[7] Tardif JC, Gregoire J, Lavoie MA, L'Allier PL. Pharmacologic prevention of both restenosis and atherosclerosis progression: AGI-1067, probucol, statins, folic acid and other therapies. Curr Opin Lipidol 2003;14:615–20.
[8] Azevedo LC, Pedro MA, Souza LC, de Souza HP, Janiszewski M, da Luz PL, et al. Oxidative stress as a signaling mechanism of the vascular response to injury: the redox hypothesis of restenosis. Cardiovasc Res 2000;47:436–45.
[9] Sawamura T, Kume N, Aoyama T, Moriwaki H, Hoshikawa H, Aiba Y, et al. An endothelial receptor for oxidized low-density lipoprotein. Nature 1997;386:73–7.
[10] Minami M, Kume N, Kataoka H, Morimoto M, Hayashida K, Sawamura T, et al. Transforming growth factor-beta(1) increases the expression of lectin-like oxidized low-density lipoprotein receptor-1. Biochem Biophys Res Commun 2000;272:357–61.
[11] Kume N, Murase T, Moriwaki H, Aoyama T, Sawamura T, Masaki T, et al. Inducible expression of lectin-like oxidized LDL receptor-1 in vascular endothelial cells. Circ Res 1998;83:322–7.
[12] Nagase M, Hirose S, Sawamura T, Masaki T, Fujita T. Enhanced expression of endothelial oxidized low-density lipoprotein receptor (LOX-1) in hypertensive rats. Biochem Biophys Res Commun 1997; 237:496–8.
[13] Chen M, Nagase M, Fujita T, Narumiya S, Masaki T, Sawamura T. Diabetes enhances lectin-like oxidized LDL receptor-1 (LOX-1) expression in the vascular endothelium: possible role of LOX-1 ligand and AGE. Biochem Biophys Res Commun 2001;287:962–8.
[14] Chen M, Kakutani M, Minami M, Kataoka H, Kume N, Narumiya S, et al. Increased expression of lectin-like oxidized low density lipoprotein receptor-1 in initial atherosclerotic lesions of Watanabe heritable hyperlipidemic rabbits. Arterioscler Thromb Vasc Biol 2000; 20:1107–15.
[15] Cominacini L, Pasini AF, Garbin U, Davoli A, Tosetti ML, Campagnola M, et al. Oxidized low density lipoprotein (ox-LDL) binding to ox-LDL receptor-1 in endothelial cells induces the activation of NF-kappaB through an increased production of intracellular reactive oxygen species. J Biol Chem 2000;275: 12633–8.
[16] Cominacini L, Fratta Pasini A, Garbin U, Pastorino A, Rigoni A, Nava C, et al. The platelet-endothelium interaction mediated by lectin-like oxidized low-density lipoprotein receptor-1 reduces the intracellular concentration of nitric oxide in endothelial cells. J Am Coll Cardiol 2003;41:499–507.

[17] Cominacini L, Rigoni A, Pasini AF, Garbin U, Davoli A, Campagnola M, et al. The binding of oxidized low density lipoprotein (ox-LDL) to ox-LDL receptor-1 reduces the intracellular concentration of nitric oxide in endothelial cells through an increased production of superoxide. J Biol Chem 2001;276:13750–5.
[18] Chen M, Masaki T, Sawamura T. LOX-1, the receptor for oxidized low-density lipoprotein identified from endothelial cells: implications in endothelial dysfunction and atherosclerosis. Pharmacol Ther 2002; 95:89–100.
[19] Oka K, Sawamura T, Kikuta K, Itokawa S, Kume N, Kita T, et al. Lectin-like oxidized low-density lipoprotein receptor 1 mediates phagocytosis of aged/apoptotic cells in endothelial cells. Proc Natl Acad Sci U S A 1998;95:9535–40.
[20] Kakutani M, Masaki T, Sawamura T. A platelet–endothelium interaction mediated by lectin-like oxidized low-density lipoprotein receptor-1. Proc Natl Acad Sci U S A 2000;97:360–4.
[21] Honjo M, Nakamura K, Yamashiro K, Kiryu J, Tanihara H, McEvoy LM, et al. Lectin-like oxidized LDL receptor-1 is a cell-adhesion molecule involved in endotoxin-induced inflammation. Proc Natl Acad Sci U S A 2003;100:1274–9.
[22] Nakagawa T, Akagi M, Hoshikawa H, Chen M, Yasuda T, Mukai S, et al. Lectin-like oxidized low-density lipoprotein receptor 1 mediates leukocyte infiltration and articular cartilage destruction in rat zymosan-induced arthritis. Arthritis Rheum 2002;46:2486–94.
[23] Aoyama T, Chen M, Fujiwara H, Masaki T, Sawamura T. LOX-1 mediates lysophosphatidylcholine-induced oxidized LDL uptake in smooth muscle cells. FEBS Lett 2000;467:217–20.
[24] Moriwaki H, Kume N, Kataoka H, Murase T, Nishi E, Sawamura T, et al. Expression of lectin-like oxidized low density lipoprotein receptor-1 in human and murine macrophages: upregulated expression by TNF-alpha. FEBS Lett 1998;440:29–32.
[25] Chen M, Kakutani M, Naruko T, Ueda M, Narumiya S, Masaki T, et al. Activation-dependent surface expression of LOX-1 in human platelets. Biochem Biophys Res Commun 2001;282:153–8.
[26] Nagase M, Hirose S, Fujita T. Unique repetitive sequence and unexpected regulation of expression of rat endothelial receptor for oxidized low-density lipoprotein (LOX-1). Biochem J 1998;330: 1417–22.
[27] Miller Jr FJ, Gutterman DD, Rios CD, Heistad DD, Davidson BL. Superoxide production in vascular smooth muscle contributes to oxidative stress and impaired relaxation in atherosclerosis. Circ Res 1998;82:1298–305.
[28] Azumi H, Inoue N, Ohashi Y, Terashima M, Mori T, Fujita H, et al. Superoxide generation in directional coronary atherectomy specimens of patients with angina pectoris: important role of NAD(P)H oxidase. Arterioscler Thromb Vasc Biol 2002;22:1838–44.
[29] Chen M, Narumiya S, Masaki T, Sawamura T. Conserved C-terminal residues within the lectin-like domain of LOX-1 are essential for oxidized low-density-lipoprotein binding. Biochem J 2001;355:289–96.
[30] Shimaoka T, Kume N, Minami M, Hayashida K, Sawamura T, Kita T, et al. LOX-1 supports adhesion of Gram-positive and Gram-negative bacteria. J Immunol 2001;166:5108–14.
[31] Iwai-Kanai E, Hasegawa K, Sawamura T, Fujita M, Yanazume T, Toyokuni S, et al. Activation of lectin-like oxidized low-density lipoprotein receptor-1 induces apoptosis in cultured neonatal rat cardiac myocytes. Circulation 2001;104:2948–54.
[32] Jono T, Miyazaki A, Nagai R, Sawamura T, Kitamura T, Horiuchi S. Lectin-like oxidized low density lipoprotein receptor-1 (LOX-1) serves as an endothelial receptor for advanced glycation end products (AGE). FEBS Lett 2002;511:170–4.
[33] Bazin-Redureau MI, Renard CB, Scherrmann JM. Pharmacokinetics of heterologous and homologous immunoglobulin G, F(ab')2 and Fab after intravenous administration in the rat. J Pharm Pharmacol 1997; 49:277–81.
[34] Caballero F, Pelegri C, Castell M, Franch A, Castellote C. Kinetics of W3/25 anti-rat CD4 monoclonal antibody. Studies on optimal doses and time-related effects. Immunopharmacology 1998;39:83–91.
[35] Hansen RJ, Balthasar JP. Pharmacokinetics, pharmacodynamics, and platelet binding of an anti-glycoprotein IIb/IIIa monoclonal antibody (7E3) in the rat: a quantitative rat model of immune thrombocytopenic purpura. J Pharmacol Exp Ther 2001;298:165–71.
[36] Li DY, Zhang YC, Philips MI, Sawamura T, Mehta JL. Upregulation of endothelial receptor for oxidized low-density lipoprotein (LOX-1) in cultured human coronary artery endothelial cells by angiotensin II type 1 receptor activation. Circ Res 1999;84:1043–9.
[37] Morawietz H, Rueckschloss U, Niemann B, Duerrschmidt N, Galle J, Hakim K, et al. Angiotensin II induces LOX-1, the human endothelial receptor for oxidized low-density lipoprotein. Circulation 1999;100: 899–902.
[38] Nagase M, Ando K, Nagase T, Kaname S, Sawamura T, Fujita T. Redox-sensitive regulation of lox-1 gene expression in vascular endothelium. Biochem Biophys Res Commun 2001;281:720–5.
[39] Rectenwald JE, Moldawer LL, Huber TS, Seeger JM, Ozaki CK. Direct evidence for cytokine involvement in neointimal hyperplasia. Circulation 2000;102:1697–702.
[40] Wolf YG, Rasmussen LM, Ruoslahti E. Antibodies against transforming growth factor-beta 1 suppress intimal hyperplasia in a rat model. J Clin Invest 1994;93:1172–8.
[41] Laporte S, Escher E. Neointima formation after vascular injury is angiotensin II mediated. Biochem Biophys Res Commun 1992;187: 1510–6.
[42] Smirnova IV, Sawamura T, Goligorsky MS. Upregulation of lectin-like oxidized low-density lipoprotein receptor-1 (LOX-1) in endothelial cells by nitric oxide deficiency. Am J Physiol Renal Physiol 2004;287:F25–32.
[43] Murase T, Kume N, Korenaga R, Ando J, Sawamura T, Masaki T, et al. Fluid shear stress transcriptionally induces lectin-like oxidized LDL receptor-1 in vascular endothelial cells. Circ Res 1998;83:328–33.
[44] Sakurai K, Sawamura T. Stress and vascular responses: endothelial dysfunction via lectin-like oxidized low-density lipoprotein receptor-1: close relationships with oxidative stress. J Pharmacol Sci 2003; 91:182–6.
[45] Tanaka K, Hayashi K, Shingu T, Kuga Y, Nomura K, Kajiyama G. Probucol inhibits neointimal formation in carotid arteries of normocholesterolemic rabbits and the proliferation of cultured rabbit vascular smooth muscle cells. Cardiovasc Drugs Ther 1998;12:19–28.
[46] Yokoyama T, Miyauchi K, Kurata T, Sato H, Daida H. Effect of probucol on neointimal thickening in a stent porcine restenosis model. Jpn Heart J 2004;45:305–13.
[47] Tardif JC, Cote G, Lesperance J, Bourassa M, Lambert J, Doucet S, et al. Probucol and multivitamins in the prevention of restenosis after coronary angioplasty. Multivitamins and Probucol Study Group. N Engl J Med 1997;337:365–72.
[48] Muscoli C, Sacco I, Alecce W, Palma E, Nistico R, Costa N, et al. The protective effect of superoxide dismutase mimetic M40401 on balloon injury-related neointima formation: role of the lectin-like oxidized low-density lipoprotein receptor-1. J Pharmacol Exp Ther 2004;311: 44–50.
[49] Fournet-Bourguignon MP, Castedo-Delrieu M, Bidouard JP, Leonce S, Saboureau D, Delescluse I, et al. Phenotypic and functional changes in regenerated porcine coronary endothelial cells : increased uptake of modified LDL and reduced production of NO. Circ Res 2000;86:854–61.

Biochem. J. (2006) 393, 107–115 (Printed in Great Britain) doi:10.1042/BJ20051166

online data

LOX-1 scavenger receptor mediates calcium-dependent recognition of phosphatidylserine and apoptotic cells

Jane E. MURPHY*‡, Daryl TACON‡, Philip R. TEDBURY*‡, Jonathan M. HADDEN†‡, Stuart KNOWLING†‡, Tatsuya SAWAMURA§, Michelle PECKHAM‡, Simon E. V. PHILLIPS†‡, John H. WALKER*‡ and Sreenivasan PONNAMBALAM*†‡[1]

*Endothelial Cell Biology Unit, Faculty of Biological Sciences, University of Leeds, Leeds LS2 9JT, U.K., †Astbury Centre for Structural Molecular Biology, University of Leeds, Leeds LS2 9JT, U.K., ‡Faculty of Biological Sciences, University of Leeds, Leeds LS2 9JT, U.K., and §National Cardiovascular Center Research Institute, Osaka 565-565, Japan

The LOX-1 (lectin-like oxidized low-density lipoprotein receptor-1) scavenger receptor regulates vascular responses to oxidized-low-density-lipoprotein particles implicated in atherosclerotic plaque formation. LOX-1 is closely related to C-type lectins, but the mechanism of ligand recognition is not known. Here we show that human LOX-1 recognizes a key cellular phospholipid, PS (phosphatidylserine), in a Ca^{2+}-dependent manner, both *in vitro* and in cultured cells. A recombinant, folded and glycosylated LOX-1 molecule binds PS, but not other phospholipids. LOX-1 recognition of PS was maximal in the presence of millimolar Ca^{2+} levels. Mg^{2+} was unable to substitute for Ca^{2+} in LOX-1 binding to PS, indicating a Ca^{2+}-specific requirement for bivalent cations. LOX-1-mediated recognition of PS-containing apoptotic bodies was dependent on Ca^{2+} and was decreased to background levels by bivalent-cation chelation, LOX-1-blocking antibodies or PS-containing liposomes. The LOX-1 membrane protein is thus a Ca^{2+}-dependent phospholipid receptor, revealing novel recognition of phospholipids by mammalian lectins.

Key words: Ca^{2+}, lectin-like oxidized low-density lipoprotein receptor-1 (LOX-1), liposomes, phosphatidylserine, protein-lipid overlay, recombinant protein.

INTRODUCTION

LOX-1 (lectin-like oxidized low-density lipoprotein receptor-1) is a mammalian scavenger receptor cloned as a receptor for OxLDL (oxidized low-density lipoprotein) [1]. LOX-1 expression can be up-regulated by pro-inflammatory stimuli including TNFα (tumour necrosis factor-α), PMA and IL-1β (interleukin 1β) [2,3] and is detected on endothelial cells, macrophages, smooth-muscle cells and platelets [4–6]. LOX-1 is implicated in the pathogenesis of atherosclerotic lesions, as OxLDL binding can trigger elevation in the levels of reactive oxygen species, monocyte chemoattractant protein-1 and matrix metalloproteinases [7–9]. LOX-1 can be detected in atherosclerotic lesions, and allelic variants are linked to the incidence of cardiovascular disease [10,11]. Furthermore, LOX-1 binds to a diverse variety of ligands, including OxLDL, apoptotic cells, activated platelets and bacteria [12–14].

LOX-1 is a structurally distinct member of the scavenger-receptor family [15] with an extracellular C-type lectin-like domain highly homologous with that of NK (natural killer)-cell receptors [16], all part of a single gene cluster on human chromosome 12 [17]. C-type lectins are classically defined as proteins that bind carbohydrate moieties in a Ca^{2+}-dependent manner [18], but NK cell receptors mediate Ca^{2+}-independent, lectin-dependent protein–protein recognition of MHC-Class I-related molecules [19,20]. The crystal structure of the LOX-1 C-type lectin-like domain reveals a lectin fold and a propensity to form homodimers [16,21].

hLOX-1 (human LOX-1) is a type II membrane protein (Figure 1A) that binds OxLDL via positively charged and neutral hydrophilic residues in the extracellular lectin-like domain [22–24], but its Ca^{2+}-dependent properties are unknown. LOX-1 has three disulphide bonds in the lectin-like domain, and the bovine orthologue can be cleaved by cellular proteases to generate a soluble extracellular LOX-1 fragment [25]. We have expressed a truncated soluble recombinant LOX-1 extracellular domain lacking the cytoplasmic and transmembrane domains and investigated its ability to bind membrane ligands. Full-length LOX-1 protein was expressed in transfected human cells to further evaluate the ability of the native protein to discriminate between ligands. We show that human LOX-1 mediates Ca^{2+}-dependent recognition of PS (phosphatidylserine) and apoptotic bodies.

EXPERIMENTAL

Reagents

All chemicals were obtained from Sigma unless otherwise stated. Mammalian- and insect-cell culture media and supplements were from Invitrogen.

Plasmids

Bacterial and baculovirus expression involved using PCR to amplify a DNA sequence encoding residues 68–273 of the extracellular domain of hLOX-1 using a complete human expressed-sequence-tag cDNA (GenBank® accession number BG547497; Geneservice). The PCR product was digested and cloned into either the pET-15b bacterial expression vector (Novagen) or a modified pTriEX1.1 insect-cell expression vector (Novagen) containing a signal sequence from the baculovirus major envelope glycoprotein gp67 (kindly provided by Dr Kevin Dalton and Professor Ian Jones, Microbiology Division, School of

Abbreviations used: ApoB-100, apolipoprotein B-100; bv-LOX-1, baculovirus/insect cell-expressed lectin-like oxidized low-density lipoprotein receptor-1; ec-LOX-1, bacterially expressed LOX-1; GST, glutathione S-transferase; His_6, hexahistidine; hLOX-1, human LOX-1; HRP, horseradish peroxidase; IL-1β, interleukin-1β; IPTG, isopropyl β-D-thiogalactoside; MOI, multiplicity of infection; Ni-NTA, Ni^{2+}-nitrilotriacetate; NK, natural killer; OxLDL, oxidized low-density lipoprotein; PC, phosphatidylcholine; PE, phosphatidylethanolamine; PI, phosphatidylinositol; PNGase F, N-glycosidase F; PS, phosphatidylserine; sTGN46, soluble His_6-tagged *trans*-Golgi-network protein 46; TBS, Tris-buffered saline; TNF-α, tumour necrosis factor-α.

[1] To whom correspondence should be addressed (email s.ponnambalam@bmb.leeds.ac.uk).

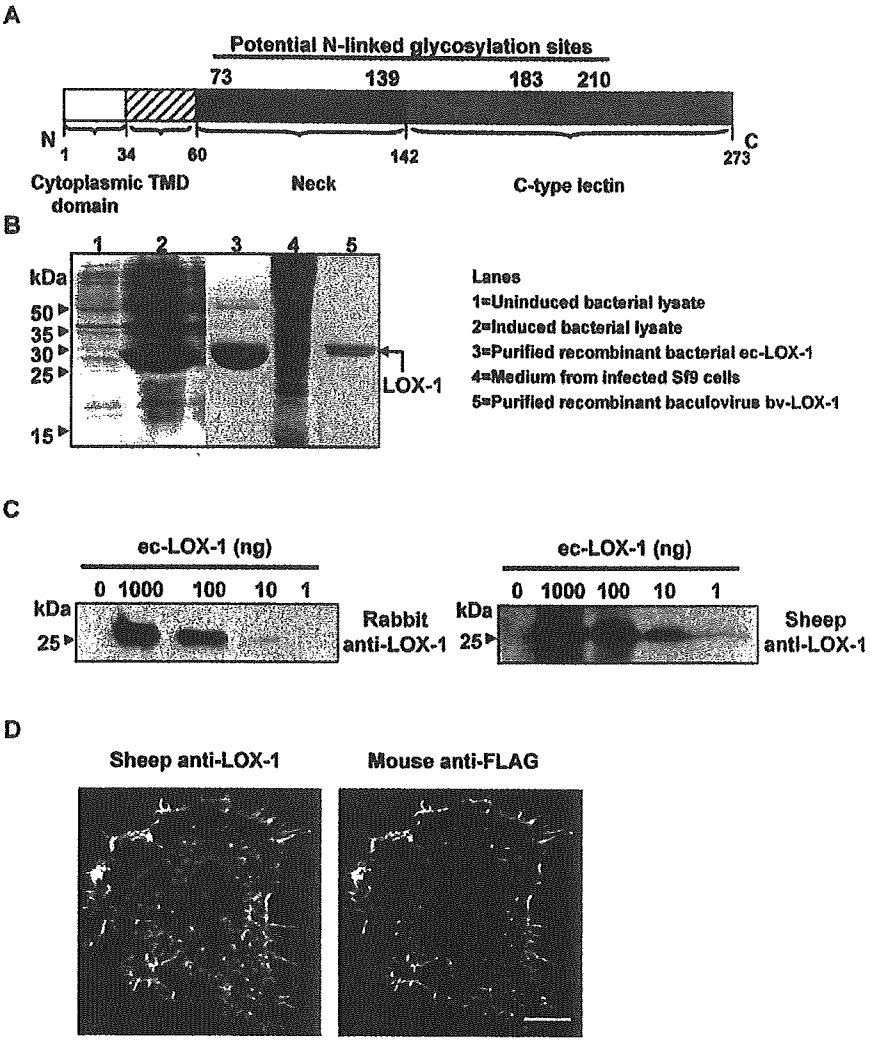

Figure 1 Expression of recombinant LOX-1 in bacteria, insect cells and mammalian cells

(**A**) Schematic representation of the domain structure of hLOX-1 (N, N-terminus; TMD, transmembrane domain; C, C-terminus). (**B**) hLOX-1 (residues 68–273) was expressed as His_6-tagged proteins in *E. coli* and Sf9 insect cells (see the Materials and methods section) and purified to produce recombinant ec-LOX-1 and bv-LOX-1 respectively. (**C**) Western blotting using recombinant ec-LOX-1 and recognition by rabbit anti-LOX-1 and sheep anti-LOX-1 antibodies. (**D**) Expression of LOX-1-FLAG construct in transfected HeLa cells. Cells were fixed and LOX-1-FLAG detected using sheep anti-LOX-1, mouse anti-FLAG and AlexaFluor-labelled secondary antibodies. Cell images represent a deconvolved, projected stack of optical sections. The scale bar represents 10 μm.

Animal and Microbial Sciences, University of Reading, Reading, Berks., U.K.). Both constructs now contained an N-terminal His_6 (hexahistidine) tag fused to the LOX-1 sequence. For mammalian-cell expression, residues 1–273 of hLOX-1 were amplified using PCR and cloned into a mammalian expression vector pCDNA3.1+ (Invitrogen) in conjunction with a FLAG peptide at the hLOX-1 C-terminus. Further details are given in the supplementary material (http://www.BiochemJ.org/bj/393/bj3930107add.htm).

Bacterial expression and protein purification

The pET-15b/LOX-1 plasmid was transformed into *E. coli* Rosetta (DE3)pLysS (Novagen). Exponential-phase cultures were induced with 0.1 mM IPTG (isopropyl β-D-thiogalactoside) at 37 °C for 6 h, pelleted by centrifugation at 4000 *g* for 30 min, and lysed in 10 mM Tris/HCl (pH 7.8)/1 mg/ml lysozyme/protease-inhibitor cocktail (Roche Diagnostics). After incubation for 30 min at 4 °C, the bacterial lysate was briefly sonicated and centrifuged at 10000 *g* for 15 min. An inclusion-body pellet was solubilized in 10 mM Tris (pH 8.0)/6 M guanidinium chloride/100 mM NaH_2PO_4 and sonicated briefly before mixing at 4 °C for 30 min. After centrifugation at 100000 *g* for 30 min, solubilized His_6-tagged LOX-1 (ec-LOX-1) was purified from the supernatant using Ni-NTA (Ni^{2+}-nitrilotriacetate)–agarose resin (Qiagen). sTGN46 (soluble His_6-tagged *trans*-Golgi-network protein 46) was produced exactly as described previously by Prescott et al. [26]. GST (glutathione S-transferase)-tagged annexin VI was produced as described by Davis et al. [27] and the GST moiety removed using thrombin protease digestion and adsorption on glutathione–agarose resin.

Insect cell expression and culture

Sf9 [*Spodoptera frugiperda* (fall armyworm)] insect cells (1×10^6) grown as a monolayer culture in six-well plates were co-transfected with 0.5 μg of pTriEx-LOX-1 and 0.15 μg of the linearized bacmid BAC10:KO_{1629} [28] (kindly provided by

Dr Kevin Dalton and Professor Ian Jones) using 8 μg of Lipofectin® (Invitrogen) in serum-free TC-100 medium at 28 °C. After 16–20 h, the DNA/Lipofectin® mix was removed and replaced with complete TC-100 medium [100 units of penicillin/ml, 100 μg of streptomycin/ml and 10 % (v/v) fetal bovine serum]. Supernatants containing recombinant baculovirus were harvested after 2–5 days incubation at 28 °C. High-titre viral stocks ($>10^9$ plaque-forming units/ml) were produced by two sequential passages in 2×10^6 Sf9 cells/ml infected at an MOI (multiplicity of infection) of 0.1. Recombinant virus amplification and protein production were carried out using suspension cultures of Sf9 cells grown in shaker flasks containing Sf-900 II serum-free medium, 100 units of penicillin/ml and 100 μg of streptomycin/ml. Large-scale cultures of Sf9 cells (1 litre) grown to a density of 2×10^6 cells/ml in serum-free medium were infected with high-titre recombinant virus at an MOI of 10 for 4 days. Cells were pelleted by low-speed centrifugation and the supernatant containing recombinant His_6-LOX-1 was incubated with 2 ml of Ni-NTA resin overnight at 4 °C. The Ni-NTA resin was washed sequentially with 50 mM NaH_2PO_4, pH 8, 300 mM NaCl, 0.05 % (v/v) Tween-20 and PBS, pH 7.4, before elution of bv-LOX-1 (baculovirus/insect-cell-expressed LOX-1) in PBS containing 250 mM imidazole. Bv-LOX-1-containing fractions were pooled and dialysed against buffer containing 20 mM sodium acetate pH 5.0, and 100 mM NaCl.

LOX-1 antibody production

Sheep and rabbits were immunized with ec-LOX-1 (bacterially expressed LOX-1) or a keyhole-limpet-haemocyanin-conjugated peptide corresponding to an extracellular hLOX-1 sequence (107–120) respectively [see the supplementary material (http://www.BiochemJ.org/bj/393/bj3930107add.htm) for further details]. Polyclonal antibodies were affinity-purified using antigen-immobilized columns.

Western blotting

Protein samples were fractionated by SDS/PAGE, transferred to nitrocellulose membranes and non-specific binding sites were blocked using 5 % (w/v) skimmed milk in PBS. Sheep anti-LOX-1 (1:1000) or rabbit anti-LOX-1 (1:1000) primary antibodies were incubated with blots for 16 h, extensively washed with PBS, followed by incubation with the appropriate anti-species HRP (horseradish peroxidase) conjugate secondary antibody (GE Diagnostics; used at 1:3000) for 2 h. Membranes were washed extensively again and bound antibodies were visualized using West Pico enhanced chemiluminescence (Perbio Science).

Far-UV CD analysis

Bv-LOX-1 was dialysed into 20 mM sodium acetate buffer, pH 5.0, at a final protein concentration of 11.3 μM, and CD measurements were recorded on a Jasco J175 spectropolarimeter over the range 200–250 nm in a 1 mm path-length cell. Spectra were obtained over a range of temperatures and blank buffer subtraction was used for averaging and baseline correction. Measurements were converted into mean residue molar ellipticity ($[\theta]_{MRW}$).

PNGase F (N-glycosidase F) digestion and analysis

Aliquots (10 μg) of bv-LOX-1 were deglycosylated using PNGase F (New England Biolabs) by incubation for either 2 or 16 h at 37 °C (see the supplementary material at http://www.BiochemJ.org/bj/393/bj3930107add.htm for further details). Controls and digested samples were subjected to SDS/PAGE and stained with Coomassie Blue.

Protein lipid overlay assay

The protein lipid overlay assay was performed essentially as described [29] in buffer containing 2 mM Ca^{2+}, Mg^{2+} or EDTA supplemented with either 100 nM bv-LOX-1, sTGN46 or annexin VI. Bound protein–phospholipid complexes were detected by incubation with sheep anti-LOX-1 (1:1000), rabbit anti-(annexin VI) (1:1000) or sheep anti-TGN46 (1:1000), followed by appropriate HRP-conjugated secondary antibodies and West Pico enhanced chemiluminescence. A Fuji Intelligent Dark Box II image reader using Fuji Las-1000 Pro software was used to capture images. Dot intensities were determined densitometrically by using Fuji Aida (Advanced Image Data Analyzer) 2.11 software. For further details, see the supplementary material at http://www.BiochemJ.org/bj/393/bj3930107add.htm.

Apoptotic-body binding assay

HeLa and HEK-293T cells were maintained in complete DMEM [with 10 % (v/v) fetal bovine serum, 100 units penicillin/ml, 100 μg streptomycin/ml, 2 mM L-glutamine and 2 mM non-essential amino acids; Invitrogen]. HeLa cells were transiently transfected using the calcium phosphate method [30]. HeLa cells grown on coverslips were transfected with pCDNA3.1/LOX-1-FLAG and incubated with apoptotic HEK-293T cells that had been treated with 1 μM staurosporine for 1 h (apoptotic bodies) in DMEM (Dulbecco's modified Eagle's medium) containing 2.5 mM Ca^{2+} at 37 °C for 30 min. To block LOX-1-mediated recognition, HeLa cells were pre-incubated with 10 μg/ml of LOX-1 blocking antibody JTX92 [9] or 10 μg/ml sheep anti-LOX-1 in DMEM for 30 min at 37 °C and washed three times with DMEM before the addition of apoptotic bodies. Synthetic liposome competition assays contained transfected HeLa cells pre-incubated with 100 μM PS or PC (phosphatidylcholine) liposomes (see the supplementary material at http://www.BiochemJ.org/bj/393/bj3930107add.htm) in TBS containing 2.5 mM Ca^{2+} for 30 min at 37 °C before addition of apoptotic bodies (also containing 100 μM PS or PC liposomes). Cells bound to apoptotic bodies were washed five times with ice-cold TBS containing 2.5 mM Ca^{2+} or three times with ice-cold TBS containing 2.5 mM EDTA, followed by two washes with ice-cold TBS containing 2.5 mM Ca^{2+}. AlexaFluor 594-labelled annexin V (Invitrogen) was diluted 1:100 in binding buffer [10 mM Hepes (pH 7.5)/140 mM NaCl/2.5 mM $CaCl_2$) and incubated with cells for 15 min at 4 °C to visualize apoptotic bodies. After washing three times with ice-cold binding buffer, cells were fixed and processed for indirect immunofluorescence microscopy [30]. To quantify apoptotic body binding, 100 LOX-1-FLAG-transfected cells were counted to assess the number of LOX-1-transfected cells with apoptotic cells (annexin V-positive bodies containing DNA) attached.

Immunofluorescence microscopy

Immunofluorescence was performed as described previously [30] (see the supplementary material at http://www.BiochemJ.org/bj/393/bj3930107add.htm). Samples were viewed using a Zeiss Axioplan II epifluorescence microscope linked to a Digital Pixel Systems CCD (charged coupled device) camera. High-resolution images were collected using a DeltaVision Optical Restoration Microscopy System (Applied Precision Inc.) and an Olympus IX-70 epifluorescence microscope. Approx. 15–20 0.2-μm-thick optical sections were collected and datasets deconvolved using the SoftWorX deconvolution algorithm. Optical sections were

projected as two-dimensional images and saved as 24-bit RGB TIFF files.

RESULTS

Recombinant LOX-1 expression

The extracellular domain of human LOX-1 (Figure 1A; residues 68–273) was expressed in both bacteria and Sf9 insect cells as His_6-tagged proteins. Recombinant bacterial LOX-1 expression was induced by IPTG (Figure 1B, lane 2) and purified as an insoluble protein (ec-LOX-1) from inclusion bodies (Figure 1B, lane 3). In contrast, insect-cell expression of bv-LOX-1 produced a soluble protein that was secreted into the extracellular medium (Figure 1B, lane 5). Secreted bv-LOX-1 was evident as a doublet on SDS/PAGE (Figure 1B, lane 5), probably corresponding to glycosylation-linked heterogeneity. Both bacterially and baculovirus-expressed recombinant LOX-1 proteins were greater than 99% pure as judged by SDS/PAGE after affinity purification on Ni-NTA–agarose resin.

Rabbit polyclonal antibodies raised to a LOX-1 peptide (residues 107–120 in the extracellular 'neck' domain) detected 0.4 pmol (10 ng) of ec-LOX-1, whereas sheep polyclonal antibodies raised to ec-LOX-1 displayed 10-fold greater sensitivity and detected 0.04 pmol (1 ng) of ec-LOX-1 (Figure 1C). The sheep antibodies also recognized bv-LOX-1 and native LOX-1 from primary human umbilical-vein endothelial cells (results not shown). We expressed the tagged hLOX-1-FLAG protein in mammalian HeLa cells with a transfection efficiency of approx. 15–20%. The transfected LOX-1-FLAG protein was simultaneously detected by both affinity-purified sheep anti-LOX-1 and mouse monoclonal anti-FLAG antibodies (Figure 1D; a colour overlay is shown in supplementary Figure S1 at http://www.BiochemJ.org/bj/393/bj3930107add.htm).

Recombinant LOX-1 folded and glycosylation state

Far-UV CD showed that the native bv-LOX-1 molecule had a folded state with pronounced minima at 208 and 222 nm (Figure 2A), indicating α-helical content. Remarkably, little difference could be detected between the CD spectra of the native bv-LOX-1 protein and the heat denatured–renatured protein (Figure 2A), indicating substantial refolding. CD analyses at increasing 5 °C intervals from 25 to 90 °C (Figure 2B) showed that the intensity of the bands at 208 and 222 nm slowly decreased with increasing temperature. However, bv-LOX-1 still exhibited a pronounced spectrum, including the 208 nm minimum (Figure 2B) at 90 °C, indicating substantial thermal stability.

PNGase F digestion showed that bv-LOX-1 is N-glycosylated at four distinct sites. PNGase F cleaves simple and complex asparagine-linked sugar moieties from a polypeptide backbone. Ec-LOX-1 and bv-LOX-1 showed an approx. 5 kDa apparent molecular mass difference on SDS/PAGE (Figure 3A). SDS/heat denaturation and PNGase F treatment of bv-LOX-1 resulted in increased SDS/PAGE mobility identical with that of ec-LOX-1, indicating that differential N-glycosylation of bv-LOX-1 produces the two polypeptides secreted into the medium (Figure 3A). Titration of PNGase F digestion caused progressively greater SDS/PAGE mobility of bv-LOX-1 (Figure 3B); partial PNGase F digestion revealed five differentially glycosylated bv-LOX-1 polypeptides (Figure 3B). Each N-linked carbohydrate attached to bv-LOX-1 effects an approx. 1–2 kDa decrease in SDS/PAGE mobility; thus the fastest migrating LOX-1 polypeptide must correspond to deglycosylated bv-LOX-1, whereas slower-migrating bv-LOX-1 forms must contain between one and four N-linked sugars.

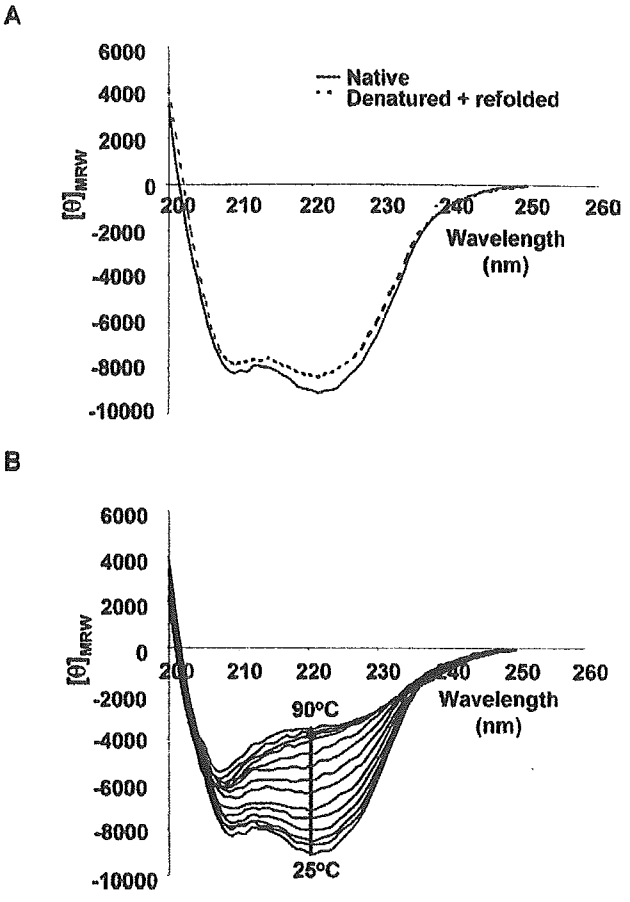

Figure 2 Far-UV CD analysis of recombinant bv-LOX-1

(**A**) Native bv-LOX-1 CD spectrum (continuous line) was measured by scanning from 200 to 250 nm at 25 °C; the 'denatured' (90 °C) and 'refolded' bv-LOX-1 CD spectrum (broken line) was measured by scanning from 200 to 250 nm at 25 °C. (**B**) Bv-LOX-1 CD spectra were measured by scanning from 200 to 250 nm at 25 °C and subsequently at increasing 5 °C intervals until 90 °C was reached. Each spectrum in (**A**) represents an average of four scans; each spectrum in (**B**) is an average of two scans. The units of $[\theta]_{MRW}$ are degrees · cm^2 · dmol^{-1}.

LOX-1 binding to phosphatidylserine is Ca^{2+}-dependent

Native LOX-1 is implicated in the recognition of apoptotic cells and activated platelets via a PS-dependent mechanism [12,13]. We tested whether this recognition is mediated by a direct interaction between LOX-1 and PS using recombinant soluble bv-LOX-1 as a probe in a protein–phospholipid overlay assay. The data showed that LOX-1 bound directly to PS (Figure 4). Comparison with a positive-control and Ca^{2+}-dependent phospholipid-binding protein, annexin VI, and a negative-control Golgi protein (sTGN46) (Figure 4A) further supported this finding. Bv-LOX-1 exhibited specificity for PS, with no binding detected to other phospholipids, including PC, PE (phosphatidylethanolamine) and PI (phosphatidylinositol) (Figure 4B).

The LOX-1 protein is part of the superfamily of C-type lectins, but there was no evidence that Ca^{2+} ions regulated ligand recognition. Binding experiments were carried out in buffers containing 2 mM Ca^{2+} to mimic physiological extracellular conditions. When we tested the Ca^{2+}-dependence of LOX-1-mediated PS recognition, we found that bv-LOX-1 bound to PS only in the presence of millimolar Ca^{2+} levels (Figure 5A). Bivalent Mg^{2+} could not substitute for Ca^{2+} in this assay (Figure 5B), further supporting the notion of a Ca^{2+}-dependent